MICROCOPY RESOLUTION TEST CHART

NATIONAL BUREAU OF STANDARDS-1963-A

(12)

INCORPORATION OF ACTIVE ELEMENTS INTO THE ARTICULATED TOTAL BODY MODEL

A. FREIVALDS

THE PENNSYLVANIA STATE UNIVERSITY
207 HAMMOND BUILDING
UNIVERSITY PARK, PENNSYLVANIA 16802

JUNE 1985

85 12 20 015

HENNING E. VON GIERKE, Dr Ing
Director
Biodynamics and Bioengineering Division
Air Force Aerospace Medical Research Laboratory

REPORT DOCUMENTATION PAGE

1a. REPORT SECURITY CLASSIFICATION	1b. RESTRICTIVE MARKINGS
Unclassified	AD-A162 518

2a. SECURITY CLASSIFICATION AUTHORITY	3. DISTRIBUTION/AVAILABILITY OF REPORT
	Approved for public release,
2b. DECLASSIFICATION/DOWNGRADING SCHEDULE	Distribution Unlimited.

4. PERFORMING ORGANIZATION REPORT NUMBER(S)	5. MONITORING ORGANIZATION REPORT NUMBER(S)
AAMRL-TR-85-061	

6a. NAME OF PERFORMING ORGANIZATION	6b. OFFICE SYMBOL (If applicable)	7a. NAME OF MONITORING ORGANIZATION
The Pennsylvania State University		Harry G. Armstrong Aerospace Medical Research Laboratory

6c. ADDRESS (City, State and ZIP Code)	7b. ADDRESS (City, State and ZIP Code)
Department of Industrial & Management Systems Engineering University Park PA 16802	Wright-Patterson AFB OH 45433

8a. NAME OF FUNDING/SPONSORING ORGANIZATION	8b. OFFICE SYMBOL (If applicable)	9. PROCUREMENT INSTRUMENT IDENTIFICATION NUMBER
US Air Force/AFSC	AAMRL	F33615-83-C-0506

8c. ADDRESS (City, State and ZIP Code)	10. SOURCE OF FUNDING NOS.			
	PROGRAM ELEMENT NO.	PROJECT NO.	TASK NO.	WORK UNIT NO.
Aeronautical Systems Division Wright-Patterson AFB, Ohio 45433	61102F	2312	V3	
	62202F	7231	23	07

11. TITLE (Include Security Classification)
See reverse side

12. PERSONAL AUTHOR(S)
Freivalds, Andris

13a. TYPE OF REPORT	13b. TIME COVERED	14. DATE OF REPORT (Yr., Mo., Day)	15. PAGE COUNT
Final	FROM 83Sep26 TO 85Jun30	1985 June 30	97

16. SUPPLEMENTARY NOTATION

17. COSATI CODES			18. SUBJECT TERMS (Continue on reverse if necessary and identify by block number)
FIELD	GROUP	SUB. GR.	Articulated Total Body Model, Biodynamics, Biokinematic Modeling, Neuromusculature
06	02		
06	07		

19. ABSTRACT (Continue on reverse if necessary and identify by block number)

The Articulated Total Body (ATB) Model, based on rigid-body dynamics with Euler equations of motion and Lagrange type constraints, is used by the Harry G. Armstrong Aerospace Medical Research Laboratory to predict the forces and motions experienced by air crew personnel in typical flight operations. To provide a more realistic representation of human dynamics, active neuromusculature was added to the ATB Model using elements of the newly developed advanced harness system.

A lumped three-parameter muscle model with a contractile element, a damping element and a parallel elastic element was developed. The contractile element included a length-tension relationship, a force-velocity relationship and an active state function. The basic fiber mechanisms were integrated into muscle systems utilizing motor unit organization, orderly recruitment of motor units and adjustments in force due to fatigue and reflex action. The complete muscle systems were then used to replicate the human neuromusculature of the trunk and neck and for the elbow, shoulder, hip and knee joints.

20. DISTRIBUTION/AVAILABILITY OF ABSTRACT	21. ABSTRACT SECURITY CLASSIFICATION
UNCLASSIFIED/UNLIMITED ☒ SAME AS RPT. ☐ DTIC USERS ☐	Unclassified

22a. NAME OF RESPONSIBLE INDIVIDUAL	22b. TELEPHONE NUMBER (Include Area Code)	22c. OFFICE SYMBOL
CORY CARROLL	(513) 255-5963	AAMRL/BBM

DD FORM 1473, 83 APR EDITION OF 1 JAN 73 IS OBSOLETE.

Block 11 continued.

Incorporation of Active Elements into the Articulated Total Body Model

Block 19 continued.

Several validation studies were performed. One simulated elbow flexion with one muscle/harness system representing the biceps brachii and the brachialis. The results indicated that the force velocity effects produced the greatest changes in force, with significant force changes due to the parallel-elastic element. Other studies simulated the whole body response to a $2G_y$ lateral force utilizing trunk musculature. Although the musculature did not completely prevent the lateral deflection of the body, the response was significantly delayed compared to a control response, with the head and neck maintaining the upright posture for a longer period of time.

PREFACE

i

TABLE OF CONTENTS

Page

.

LIST OF FIGURES

LIST OF TABLES

LIST OF SYMBOLS

A   =   cross-sectional area of muscle

B   =   viscous damping coefficient

BE   =   cross-bridge elastic element

CE   =   contractile element

DE   =   damping element

E   =   viscoelastic spring constant

f   =   force developed in muscle normalized by the maximum isometric tension

f_{DE} =   force developed by damping element normalized by the maximum isometric tension

f_{ℓ} =   force due to length-force relationship normalized by the maximum isometric tension

f_{PE} =   force developed by parallel elastic element normalized by the maximum isometric tension

f_v = force due to force-velocity relationship normalized by the maximum isometric tension

F = force developed in muscle

F_{MAX} = maximum isometric tension

K_{PE} = spring constant for parallel elastic element

K_{SE} = spring constant for series elastic element

ℓ = instaneous muscle length

ℓ_0 = resting muscle length

m = mass

n = relative number of recruited motor units

n_I = relative number of Type I motor units

n_{II} = relative number of Type II motor units

N = number of recruited motor units

N_I = number of Type I motor units

N_{II} = number of Type II motor units

$\bar{N}$ = total number of motor units

NF   = functional form for muscle model

p   = rate of change of active state

PE   = parallel elastic element

PS   = parallel elastic element of the sarcolemma

q   = active state function

s   = slack in muscle length

SE   = series elastic element

t   = time

t_c = contracation time of motor unit

t_{end} = endurance time

γ = $\gamma_f - \gamma_o$

γ_o = resting Ca^{++} concentration

γ_f = free Ca^{++} concentration

ε = muscle strain

$\dot{\varepsilon}$ = muscle strain rate

$\dot{\varepsilon}_{MAX}$ = maximum muscle strain rate

ε' = pretensioned muscle strain

n = viscous damping coefficient

$\dot{\eta}$ = normalized muscle velocity

λ = length of contractile element

$\bar{\lambda}$ = resting length of contractile element

$\dot{\bar{\lambda}}_0$ = maximum shortening velocity of contractile element

λ_B = length of cross bridge elastic element

λ_S = length of series elastic element

μ = microns

ν = relative stimulation rate

ξ = normalized length of contractile element

τ^{-1} = stimulation rate

$\bar{\tau}^{-1}$ = maximum stimulation rate

I. INTRODUCTION

Biodynamic computer-based models for the prediction of human body
response to mechanical stress have become extremely useful and cost-effective
research and developmental tools, especially as alternatives to direct
experimentation with humans and animals. These models attempt to simulate or
predict the forces and motions experienced by a body in high-acceleration
events such as impacts or from sudden forces such as wind shear. In
particular, the Air Force is interested in the reactions of aircrew personnel
to such forces typically encountered in various phases of flight operations,
including emergency ejections from high-speed aircraft. Such a hazardous
environment is well suited to computer modeling, and with proper execution,
considerable insight into body motion and stresses developed in the body can
be gained.

The Modelling and Analysis Branch of the Biodynamics & Bioengineering
Division of the Air Force Aerospace Medical Research Laboratory (AFAMRL) has
been using a human body modelling computer program known as the Articulated
Total Body (ATB) Model for several years. The model is based on rigid-body
dynamics using Euler equations of motion with Lagrange-type constraints (Fleck
et.al. 1974). The specific configuration uses 15 body segments (head, neck,
upper torso, center torso, pelvis, upper arms, lower arms, upper legs, lower
legs, and feet) and 14 joints between the segments (Fleck and Butler, 1975).
Although it was originally developed by the Calspan Corporation for the study
of human-body and anthropometric-dummy dynamics during automobile crashes for
the United States Department of Transportation (Fleck et.al. 1974; Fleck,
1975), the ATB Model was sufficiently general to allow simulation of
whole-body articulated motion resulting from various impacts or abrupt
accelerations applied to the body. Furthermore, modifications involving

1

special joint forces, aerodynamic forces and a complex harness system were added to accommodate specific Air Force applications (Fleck and Butler, 1975).

The ATB Model initially reflected human body structure, mass distribution and tissue material properties for passive responses. An early effort to improve the ATB Model in regards to active responses resulted in the development of a lumped three parameter viscoelastic muscle model superimposed on the advance restraint system. (Freivalds, 1984; Freivalds and Kaleps, 1983; Freivalds and Kaleps, 1984). However, the early efforts were constrained by the low number (five) of harness systems provided in the ATB Model, limiting simulations to simple joint motions or very crude whole body motion. Also, complex neuromuscular functions such as motor unit recruitment patterns, time varying effects, etc. were not included. Thus, further development of the neuromuscular system was needed to better simulate active human responses to high G forces.

II. OBJECTIVES

The objective of this project was to further define and formulate methodologies for implementing active muscle responses into the present ATB Model. Three considerations were involved: (1) basic muscle phenomena such as motor units, recruitment patterns, and fatique were to be included, (2) particular emphasis was to be placed on muscles acting in the torso and neck region which affect flexion, extension and lateral motion of the trunk in a seated posture and (3) the modifications should be transparent to the user, such that existing input decks would remain valid.

The objective was approached in four-phased approach. In Phase I, the basic muscle model developed during the early efforts (Freivalds, 1982; Freivalds, 1984), was re-examined and redefined. In Phase II, advanced features of types of motor unit, motor unit recruitment, force buildup and

2

endurance times were developed and included into the ATB Model. In Phase III, the ATB Model was modified to allow for up to 50 muscles and a representative musculature for the entire body was developed. In Phase IV, various simulations were performed in order to validate the modelling efforts.

III. BACKGROUND

A. Skeletal Muscle:

Skeletal muscles usually originate on the skeleton, span one or more joints and insert into a part of the skeleton again. Each muscle is enclosed in a connective tissue sheath called the epimysium and is held in its correct position in the body by layers of fascia. The muscle is attached to the bones via tendons, while the interior is compartmentalized into longitudinal sections called the fasciculi, each containing many individual muscle fibers. The fibers are enveloped by a connective tissue called the endomysium, which transmits the force of the muscle contraction from individual fibers to the tendons (Fung, 1981).

The muscle fibers do not always run parallel to the force transmitting tendons, as they do in fusiform muscles. They can be arranged in unipennate, bipennate or multipennate form, thus altering the force transmittinig characteristics (Fig. 1).

The muscle fiber, the basic structural unit, with a diameter of 10-60 μ and length from several millimeters to several centimeters, can be subdivided further into myofibrils of 1μ diameter. These myofibrils comprise the hexagonal array of protein filaments that are directly reponsible for the contractile process and give rise, with appropriate stains to the peculiar striations that are characteristic of skeletal muscle (Figure 2). A repeating unit known as the sarcomere is defined by the vertical z-disk. Two types of

3

UNIPENNATE   BIPENNATE   MULTIPENNATE
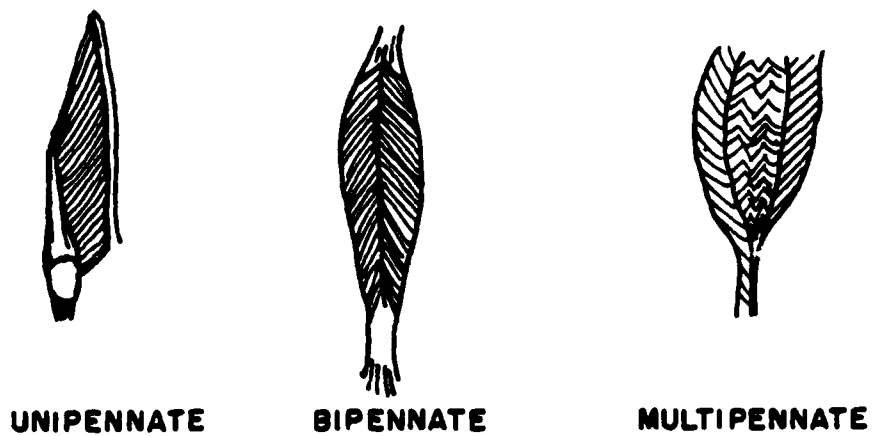
Fig. 1   Schematic representation of skeletal
muscle fibre arrangement.
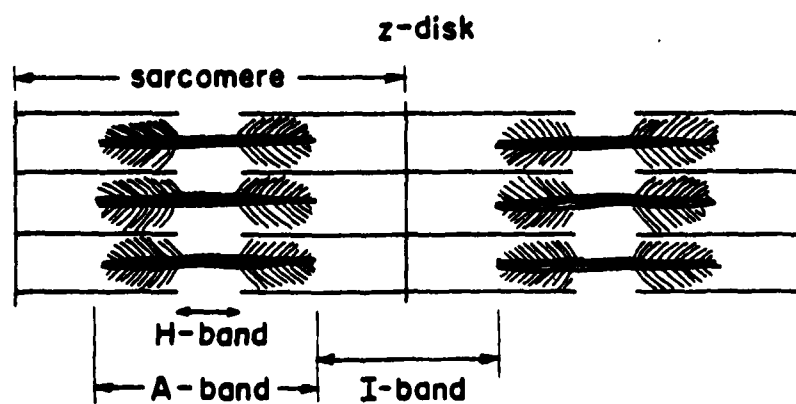
Fig. 2   Molecular substructure of mammalian
skeletal muscle.

4

protein filaments are distinguishable in each sarcomere, thin ones about 5nm (50Å) in diameter and thicker ones about 12nm (120Å) across. The thin filaments contain actin, globular molecules in a triple helix, while the thick filaments contain myosin, long molecules with globular heads. The thin filaments are each attached at one end to a z-disk and are free at the other to interlace with the thick filaments. The A-band is the region of overlap between thick and thin filaments, the I-band contains solely the thin filaments, while the H-band is the middle region of the A-band into which the actin filaments have not penetrated (Fung, 1981).

The actual contractile process takes place at the junctions between the myosin and actin in a process known as the sliding filament theory first presented by H. E. Huxley (1953). The myosin molecules consist of a long tail piece and a "head". The tails lie parallel in a bundle to form the core of the thick filament while the heads project laterally from the filament in pairs, rotated with respect to its neighbors to form a spiral pattern along the filament. These heads seem to be able to nod; they lie close to their parent filament in relaxation, but stick out to actin filaments when excited. Thus, during muscle contraction the muscle fiber shortens as the filaments slide over each other, forming, breaking and reforming chemical bonds between the myosin heads and the globular actin molecules.

B. Passive Viscoelastic elements:

Previous modelling efforts (Freivalds, 1982; Freivalds, 1984; Freivalds and Kaleps, 1983; Freivalds and Kaleps, 1984) produced the lumped model of skeletal muscle shown in Figure 3. Structures which lie in parallel to the force producing sarcomeres: the sarcolemna (sheath) of the individual fiber and the various outer connective sheaths (fascia, endomysia, perimysia) are represented by the parallel elastic element (PE). Practically all the tension

5

observed when stretching the resting muscle will result from this element. Because the muscle fiber is 60% water, an appropriate damping element (DE) is also included parallel to the contractile elements (CE). The contractile element represents the purely contractile protein molecules. In series with the contractile element is a bridge element (BE) representing the elastic elements within the cross bridges and the z-disks. The parallel elastic element for the sarcomere (PS) does not contain a damping component, since the sarcolemma attached to the z disks does not allow appreciable movement. The tendinous parts of the muscle fiber are located near the origin and insertion of the fiber and thus are depicted by a series elastic element (SE). Any mass of the sarcomeres is disregarded, especially when compared to the much larger external mass that the muscle contraction must move (Hatze, 1981).

Certain assumptions allow a further reduction of the lumped model to a simpler model yet. SE and BE can be considered to be very stiff springs and eliminated completely. This contention is supported by Bawa et.al. (1976) who found $K_{SE}=3724$ N/m to be much larger than $K_{PE}=1000$ N/m. K_{BE} can be considered to be in a similar range with K_{SE}. Eliminating SE and BE results in a model with four parallel elements, two of which are elastic and can be combined into one parallel elastic element. The final simplified model is given in Figure 4.

The total force developed by the simplified model of Figure 4 can now be expressed as:

$$F = (f_{PE} + f_{CE} + f_{DE})F_{MAX} \qquad (1)$$

where F_{MAX} is the maximum isometric tension of the muscle.

6
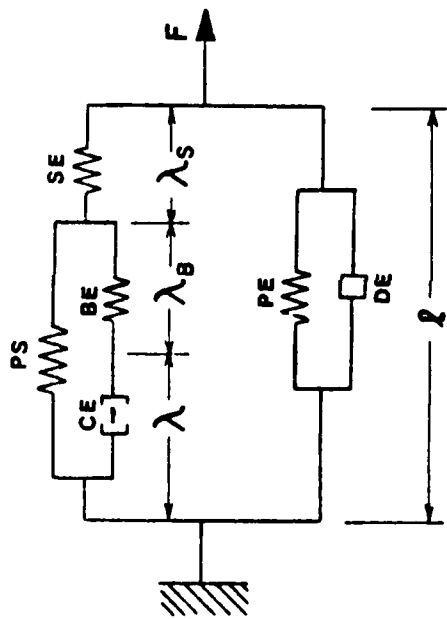
Fig. 3   Lumped model of skeletal muscle.
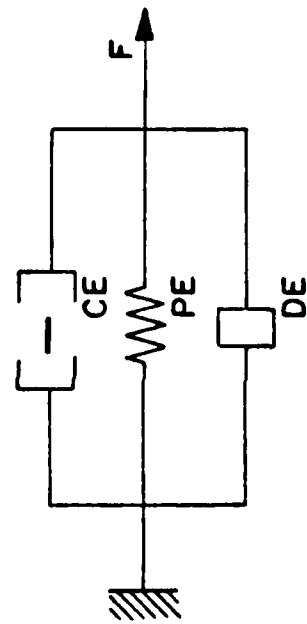
Fig. 4   Simplified muscle model.

7

For concentric or shortening contractions both f_{PE} and f_{DE} are zero, PE producing force only under stretch and DE producing force only under external tension, i.e. eccentric motion.

Mathematical representations for each element were determined as follows. For the parallel elastic element, extensive tests on the tensile properties of resting human sartorius muscle carried out by Yamada (1970) indicate an exponential force-strain function:

$$f_{PE} = .0016296(e^{7.6616\varepsilon}-1) \qquad (2)$$

where f_{PE} is the force developed by the PE normalized with respect to maximum isometric tension in the muscle and ε is the strain:

$$\varepsilon = \frac{\ell - \ell_o}{\ell_0} \qquad (3)$$

where ℓ is the instananeous muscle length and ℓ_o is the resting length. This force-strain curve is shown in Figure 5.

The velocity dependence of the damping element (DE) can be expressed similarly to the form used for a simple mechanical dashpot:

$$f_{DE} = \eta \, \dot{\varepsilon} \qquad (4)$$

where f_{DE} is the normalized force, $\dot{\varepsilon}$ is the muscle strain rate and η is the viscous damping coefficient. As mentioned previously (Freivalds, 1984) the force produced by the passive viscous damping element, amounted to as much as a 30% increase above MVC. This seemed to be an excessively large effect for a passive response and consequently the damping coefficient was re-evaluated. Alexander and Johnson (1965) loaded the frog sartorius muscle dynamically in both the passive and active states. From the ramp shaped

8

Fig. 5 PASSIVE MUSCLE FORCE —STRAIN FUNCTION

f_{PE}

MUSCLE STRAIN — ϵ

9
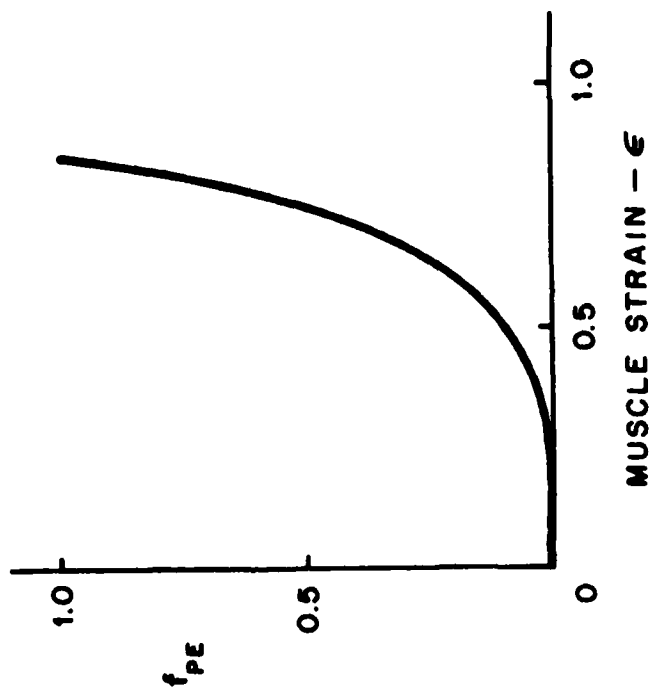
loading curves one can establish time constants for the resulting strain
responses as follows. Using viscoelastic modelling techniques (Bland, 1960;
Flugge, 1967) one can express the relationship of a parallel combination of a
spring and dashpot as:

$$\sigma(t) = E\epsilon(t) + \eta\dot{\epsilon}(t) \tag{5}$$

where σ = stress, and E = spring constant. Taking the Laplace transform of
both sides yields:

$$\sigma(s) = (E + \eta s)\ \epsilon(s) \tag{6}$$

If the loading function is a ramp function of the form $\sigma_0 t$, then its Laplace
transform is σ_0/s^2 and the resulting strain becomes:

$$\epsilon(s) = \frac{\sigma_0}{s^2(E+\eta s)} \tag{7}$$

Through partial fraction expansion the strain becomes:

$$\epsilon(s) = \frac{\sigma_0}{\eta}\ \left(\frac{\eta}{Es^2}\ \frac{-\eta^2}{E^2 s}\ +\ \frac{\eta^2}{E^2(s + E/\eta)} \right) \tag{8}$$

The inverse Laplace transform yields the expression:

$$\epsilon(t) = \sigma_0\ \left(\frac{t}{E} - \frac{\eta}{E^2}\ (1 - e^{-E/\eta\ t}) \right) \tag{9}$$

Based on the work of Alexander and Johnson (1965), the strain n in Eq. 9
can be considered a composite strain consisting of a dynamic strain and a
passive strain. At time t equal 4 sec, the resulting elongation from a

10

linear ramp loading of 4.4 gr/sec is .5 mm for the passive state and .075 mm

for the active state. In the passive state the viscous damping forces for

both the contractile element and secondary tissues come into play. During the

active state the damping effect in the contractile element is overshadowed by

the force velocity relationship and only the damping effect due to other

tissues is measured. Based on the data of the frog sartorius E = 6.57 gr/sec,

σ_0 = 4.4 gr/sec, t = 4 sec). Alexander and Johnson (1965) found a value of

6.38 for the ratio of the combined damping coefficient (found during

the passive state) to the passive damping coefficient (found during active

state).

Converting the cat plantaris combined damping coefficient of 63 Nsec/m

(which is more similar to human values as opposed to the frog coefficient)

found by Bawa, Mannard and Stein (1976) yields a value of 9.87 Nsec/m.

Normalizing to the plantaris length of .05 m and maximum contraction force of

2.45 N yields the final passive damping coefficient value of .139 sec. The

complete functional relationship of Eq. 4 is plotted in Fig. 6. Note that

damping is only effective on eccentric movements.

C. Active Muscle Elements:

The contractile element is the only active component in the model. Its

behavior is extremely complex and depends nonlinearly on its length,

contractive history, velocity of movement, the degree of stimulation and its

temperature. However, for practical purposes, only three basic functions were

considered: the length-force relationship (f_ℓ), the force-velocity

relationship (f_v), and the active state function (f_q). Thus

$$f_{ce} = f_q \cdot f_\ell \cdot f_v \tag{10}$$

11

Fig. 6 PASSIVE MUSCLE VISCOUS DAMPING FORCES
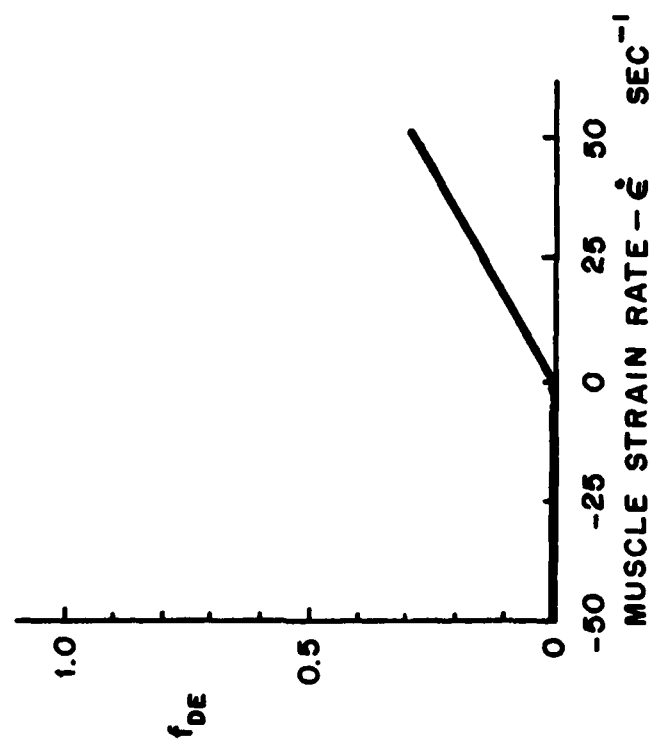
The length-force relationship is determined by the number of active cross links or filamentary overlap and can be adequately expressed from the data of Gordon et.al. (1966) by the function suggested by Hatze (1981, p. 42):

$$f_\ell(\epsilon) = .32 + .71e^{-1.112\epsilon} \sin(3.722(\epsilon+.344)) \tag{11}$$

This function is shown in Figure 7 and further details are given in Freivalds (1982).

The force-velocity relationship is determined by the rate of breaking and reforming the cross bridges with higher rates producing less effective bonds. To account for the whole range of negative velocities (shortening or concentric contractions) as well as positive velocities (lengthening or eccentric contractions) Hatze (1981, p. 45-46) has defined the following expression:

$$f_v(\dot{\eta}) = .1433 \left\{ .1073 + e^{-1.409} \sinh (3.2\dot{\eta} + 1.6) \right\}^{-1} -.005[2-e^{6\epsilon}] \tag{12}$$

where $f_v(\dot{\eta})$ is the normalized force due to the force-velocity relationship as defined by the first term and reduced by internal resistance as defined by the second term. However, since the coefficient of the second term is smaller by a factor of 30 than the first term, it can be disregarded for present purposes. $\dot{\eta}$ represents the normalized contractile element velocity:

$$\dot{\eta} = \dot{\epsilon}/\dot{\epsilon}_{MAX} \tag{13}$$

with $\dot{\epsilon}_{MAX}$ being the maximum shortening velocity of the contractile element. Equation 6 represented by Figure 8, with further details given in Freivalds (1982).

13

Fig.7 MUSCLE LENGTH-FORCE
RELATIONSHIP

f_L

MUSCLE STRAIN — $\in$

14
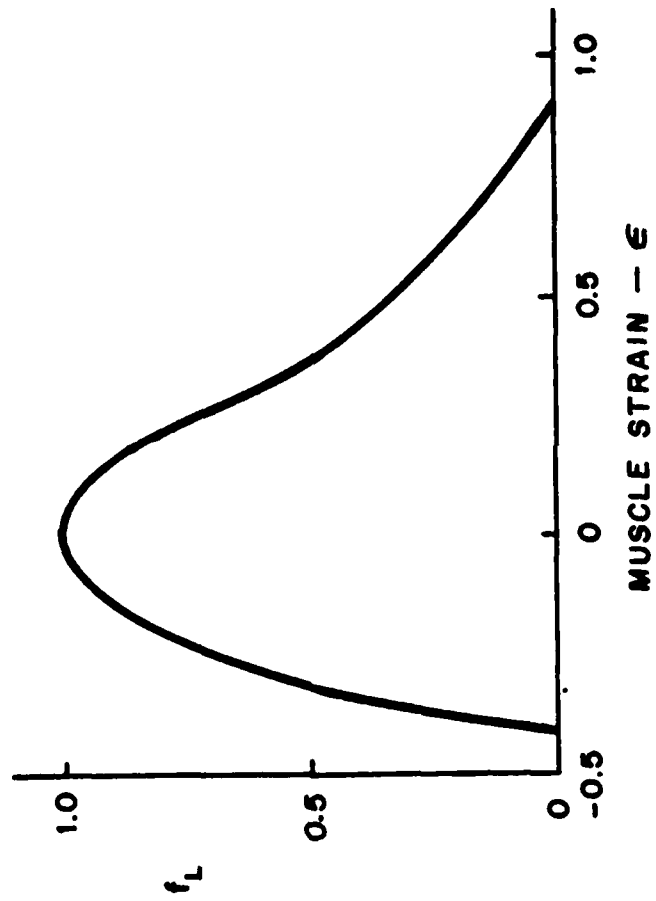
Fig. 8 MUSCLE FORCE—VELOCITY RELATIONSHIP

$$\dot{n} = \frac{\dot{\epsilon}}{\dot{\epsilon}_{MAX}}$$
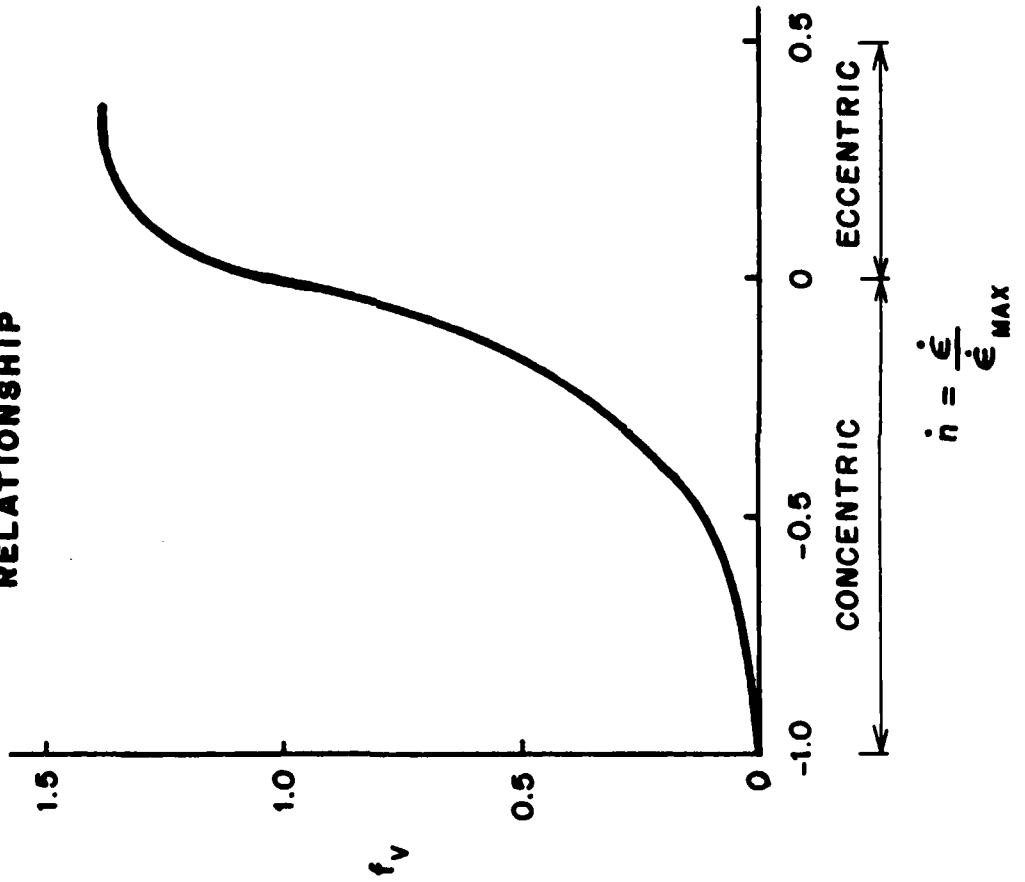
The active state function f_q is defined by the relative amount of calcium (Ca^{++}) bound to troponin (inhibitor molecule of actin). If the maximum number of potential interactive sites on the thin filament are exposed by the action of Ca^{++}, then $q=1$; while in a resting state $q=q_0$. Thus the isometric tension developed by a muscle fiber at a given length ℓ_q the CE is directly proportional to q (Hatze, 1981, p. 33).

Define Υ to be the difference between the real free Ca^{++} concentration Υ_f and the free Ca^{++} concentration Υ_0 in the resting fiber. However, for practical purposes since $\Upsilon_0 \ll \Upsilon_f$, we have $\Upsilon = \Upsilon_f$. Let $p = dq/d\Upsilon$ denote the Ca^{++} concentration rate of change of the active state q. The process of binding Ca^{++} ions to the troponin sites is hypothesized by Hatze (1981) and supported by the experimental studies of Ebashi and Endo (1968) to be a function of the length ℓ of the CE and of the difference between the maximum and present value of q and controlled by a negative feedback loop as follows.

$$dp/d\Upsilon = \rho_1^2(\epsilon)\ (1-q) - 2\rho_2\rho_1(\epsilon)p \qquad (14)$$

where $\epsilon = (\ell - \ell_0)/\ell_0$ is the strain and

$$dq/d\Upsilon = p \qquad (15)$$

Solving the differential system of Equation 14 and Equation 15 with initial conditions:

$$p(0) = 0 \qquad (16)$$
$$q(0) = q_0 = .005 \qquad (17)$$

One obtains a normalized solution:

16

$$q(\epsilon,Y) = 1 - \frac{(1-q_0)}{(m_1-m_2)} \quad m_1 e^{m_2 \rho_1(\epsilon)Y} - m_2 e^{m_1 \rho_1(\epsilon)Y} \tag{18}$$

where

$$m_{1,2} = -\rho_2 \pm (\rho_2^2 - 1)^{1/2} \quad \rho_2 > 1 \tag{19}$$

Substituting experimentally found values (Hatze, 1981):

$$\rho_1^2 = 2.34 \times 10^{14} \left(\frac{\epsilon + .44}{\epsilon + 1}\right)^{1/2} \quad -.44 \leq \epsilon \leq .8 \tag{20}$$

$$\rho_2 = 1.05 \tag{21}$$

One obtains:

$$q(\epsilon,Y) = 1 - (1-q_0)(2.14 \ e^{-1.167 \times 10^7 h(\epsilon)Y(t)} \tag{22}$$

$$-1.14 e^{-2.096 \times 10^7 h(\epsilon)Y(t)})$$

where $\tag{23}$

$$h(\epsilon) = \left(\frac{\epsilon + .44}{\epsilon + .1}\right)^{1/2}$$

However, a simple computational approximation is provided by Hatze (1981, p. 40) for most mammalian muscles:

$$q(\epsilon,Y) = \frac{q_0 + \rho^2(\epsilon)Y^2}{1 + \rho^2(\epsilon)Y^2} \tag{24}$$

where

$$\rho(\epsilon) = 66,200 \ \frac{1.9(\epsilon + 1)}{1.9 - \epsilon} \tag{25}$$

17

The function γ, the free Ca^{++} ion concentration can be represented as a function of time t and the stimulation rate ν by a trend function which represents the average behavior of γ in successive time intervals, and which approaches a maximum value asymptotically and has the rate of increase proportional to the stimulation rate (Hatze, 1981, p.39).

$$\dot{\gamma} = m(C\nu - \gamma) \quad \gamma(0) = \gamma_0 \tag{26}$$

where m and C are constants ($C = 1.373 \times 10^4$ (Hatze, 1981) and m to be determined later) and ν is the relative stimulation rate defined by

$$0 \leq \nu = \frac{\bar{\tau}}{\tau} \leq 1 \tag{27}$$

where τ^{-1} and $\bar{\tau}^{-1}$ denote the stimulation rate and maximum stimulation rate respectively.

The rate of stimulation of motor units during voluntary contraction has been very controversial. Several studies have found a fairly constant discharge frequency over a wide range of tension for individual motor units (Bigland and Lippold, 1954; Clamann, 1970), while others maintain that an increase in muscle tension is achieved in part by an increase in the stimulation rate and that this may be important in achieving precision and smoothness of contraction (Marsden et.al 1971; Person and Kudina, 1972; Milner-Brown et.al 1973b). However, even for those studies who found a rise in discharge frequency with tension, the frequency at the start of the discharge for rapid contractions was much higher and closer to the maximum stimulation rate (Tanji and Kato, 1973). Thus, it is fairly reasonable to assume a constant stimulation rate and, therefore, a constant relative stimulation rate.

18

Now solving Equation 26 with ν constant yields:

$$\gamma = (\gamma_0 - C\nu) \, e^{-mt} + C\nu \tag{28}$$

With $\gamma_0 \ll C\nu$ ($\gamma_0 = 1 \times 10^{-9}$; Hatze, 1981, p. 33), Equation 28 reduces to:

$$\gamma = C\nu(1 - e^{-mt}) \tag{29}$$

Substituting Equation 29 and Equation 25 (with $\epsilon = 0$) into Equation 24 yields the active state function:

$$q(t) = \frac{.005 + 82.63 \; \nu^2 \; (1-e^{-mt})^2}{1 + 82.63 \; \nu^2 \; (1-e^{-mt})^2} \tag{30}$$

which is represented in Fig. 9. Consequently, f_{CE} can be redefined by using the relative force f_q developed by the active state function q:

$$f_{CE} = f_q(t) \; f_\ell(\epsilon) \; f_v(\dot{\eta}) \tag{31}$$

IV. PHASE II - ADVANCED DEVELOPMENT

A. Organization of Fibers into Motor Units

The population of motor units can be subdivided into two distinct populations based on their contractile and histochemical properties: Type I (slow twitch) motor units and Type II (fast twitch) motor units (Close, 1972). Type I motor units have slower contraction times, tend to be more aerobic and less fatigable and are recruited at lower tension levels. Type II motor units have faster contraction times, tend to be more anaerobic and more fatigable and are recruited at higher tension levels (Close, 1972; Milner - Brown, et.al., 1973a). Thus, the total muscle force output should be the sum of the

19

Fig. 9 RELATIVE FORCE DEVELOPED BY ACTIVE STATE FUNCTION VS. TIME

KEY

TYPE II M.U., REL. STIM. = 1
TYPE II M.U., REL. STIM. = 0.5
TYPE I M.U., REL. STIM. = 1
TYPE I M.U., REL. STIM. = 0.5

TIME — sec

RELATIVE ACTIVE STATE FUNCTION
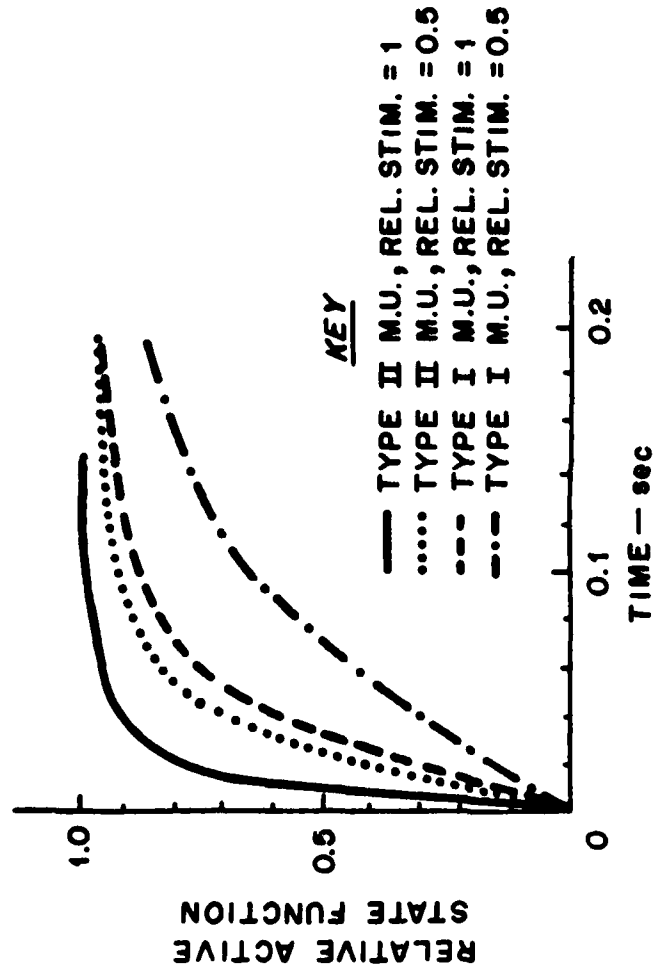
force output from N_I of the Type I motor units and N_{II} of Type II motor units:

$$F = (f_{PE} + f_{CE_I} + f_{CE_{II}} + f_{DE})F_{MAX} \qquad (32)$$

Furthermore, the same total population can be subdivided into two-dynamically different populations: the N population of active motor units and the $\bar{N}$-N population of inactive or resting motor units, where $\bar{N}$ is the total number of motor units in the muscle.

Muscle properties dependent on fiber type will be developed in the next section as many of these also depend on the recruitment pattern used.

B. Orderly Recruitment of Motor Units

It has been well established that motor units are recruited in a sequential order according to their sizes (Milner - Brown, et.al. 1973a). The cumulative relative cross-sectional area u occupied by the fibers of the recruited units increases by:

$$u = u_o \, e^{\bar{c} \frac{(N-1)}{\bar{N}}} \qquad o < u_o < u \leq 1 \qquad (33)$$

where u_0 is the cross-sectional area of the smallest motor unit,

$$\bar{c} = -\ell n \, u_o, \qquad (34)$$

N is the number of stimulated motor units and $\bar{N}$ is the total number of motor units (Hatze, 1979). For $\bar{N}$ large, Equation 24 reduces to:

21

$$u_n = u_o e^{\bar{c}N/\bar{N}} = u_o^{(1-N/\bar{N})} = u_o^{(1-n)} \tag{35}$$

where n is the normalized number of recruited or active motor units = $N/\bar{N}$.

The $\Delta_i u$ of the relative cross-sectional area u upon recruitment of the ith motor unit is then defined by:

$$\Delta_i u = C \, e^{\bar{c}_i/\bar{N}} \tag{36}$$

where C is a normalization constant determined by the requirement that

$$\sum_{i=1}^{\bar{N}} \Delta i u = 1 \quad i.e.$$

$$C = \frac{1}{\displaystyle\sum_{i=1}^{\bar{N}} e^{\bar{c}_i/\bar{N}}} \tag{37}$$

Applying the ratio of the smallest to the largest motor cross-sectional areas measured in a muscle, an estimate of the value of u_o for a given muscle can be found. These range from $u_o = .005$ for the human rectus femorus muscle to $u_o = .009$ for the human biceps muscle (Hatze, 1979) with an average value of $u_o = .00673$ resulting in $\bar{c} = 5$ to be used for the present study.

Thus two very important properties of motor unit recruitment dynamics have been included; motor units are normally recruited sequentially from the smallest to the largest and the size of the recruited units as well as the total force produced grows exponentially (Fig. 10). Combining the two sets of overlapping population distribution of motor units yields two distinct cases:

Fig. 10   FORCE DEVELOPED BY ORDERLY RECRUITMENT OF MOTOR UNITS

RELATIVE TOTAL FORCE

RELATIVE NUMBER OF MOTOR UNITS RECRUITED
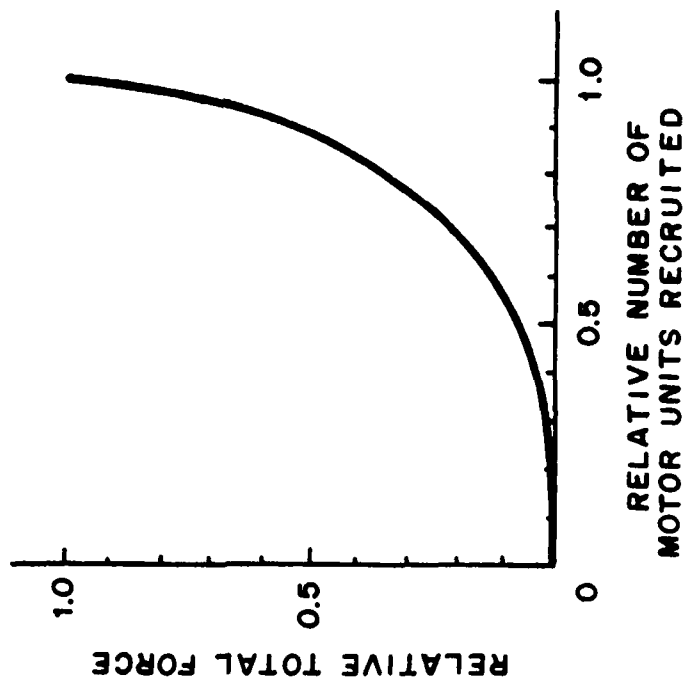
a) $N < N_I$, ie. only part of the Type I motor units are stimulated and none of the Type II can be stimulated because of the orderly recruitment pattern and b) $N > N_I$, ie., all Type I motor units are stimulated and some of the Type II motor units are stimulated, but none of the Type I are inactive. These conditions are included for the muscle properties for which they are appropriate.

Appropriate properties of motor units can be obtained from the data presented in Henneman and Olson (1965). The contraction time t_c of a motor unit is a decreasing function of the fraction n of recruited motor units:

$$t_c = a_2 - a_3 n \tag{38}$$

Thus for Type I motor units

$$t_{c_I} = a_{2_I} - a_{3_I} n \qquad 0 \leq n \leq n_I \tag{39}$$

and for Type II motor units

$$t_{c_{II}} = a_{2_{II}} - a_{3_{II}} n \qquad n_I \leq n \leq 1 \tag{40}$$

The constants a_{2_I}, a_{3_I}, $a_{2_{II}}$, $a_{3_{II}}$ can be determined from experimental values. For n=0, the value of t_c corresponds to the contraction time of the slowest Type I unit in the muscle, approximatley equal to .1 sec.; for n=n_I the value of t_c corresponds to the fastest Type I unit, approximately .045 sec.; and for n=1 (given n_I=1) the value of t_c corresponds to the fastest Type II unit, approximately .01 sec. (Grimby and Hannerz, 1977). Substituting and solving for the unknown values yields:

24

$$a_{2_I} = .1 \tag{41}$$

$$a_{3_I} = .055/n_I \tag{42}$$

$$a_{2_{II}} = .01 + \frac{.035}{(1-n_I)} \tag{43}$$

$$a_{3_{II}} = \frac{.035}{(1-n_I)} \tag{44}$$

Substituting Equations 41 and 42 into Equation 39 and Equations 43 and 44 into Equation 40 yield respectively:

$$t_{C_I} = .1 - .055 \frac{n}{n_I} \qquad 0 \le n \le n_I \tag{45}$$

$$t_{C_{II}} = .01 + .035 \frac{1-n}{1-n_I} \qquad n_I \le n \le 1 \tag{46}$$

Several other important parameters can be derived using Equations 45 and 46. Close (1965) showed that *for mammalian skeletal muscle the maximum normalized speed of shortening is related to the contraction time of a muscle, consisting predominantly of one fiber type,* by:

$$\dot{\epsilon}_{MAX} = \frac{B}{t_c} \tag{47}$$

where B has a value of .297 for human muscle. Using Equations 45, 46 and 47, $\dot{\epsilon}_{MAX}$ is found to be 2.97/sec. for slow (n=0) and 29.7/sec. for fast (n=1) motor units. However, for present modelling purposes, an average value for $\dot{\epsilon}_{MAX}$ will be used. Integrating t_c from Equation 45 over the pattern of motor unit recruitment for Type I motor units (with $\bar{c}$ = 5 for human muscle):

$$t_{C_I} = \frac{\int_0^n \frac{(.1 - .055x)}{n_I} e^{\bar{c}x} dx}{\int_0^n e^{\bar{c}x} dx} \tag{48}$$

25

yields:

$$t_{C_I} = \frac{.1(e^{5n}-1) - \frac{.011}{n_I}\ e^{5n}(5n-1)-1}{e^{5n}-1} \qquad (49)$$

A similar process of integrating over the pattern of Type II motor

unit recruitment yields an average contraction time of

$$C_{II} = .01 + \frac{.035}{1-n_I} - \frac{\frac{.007}{(1-n_I)}\left(e^{5}n(5n-1) - e^{5}(5n_I-1)\right)}{\left(e^{5n} - e^{5n_I}\right)} \qquad (50)$$

The rate constant in Equation 29 also depends on the contraction

time:

$$m = A_0/t_C \qquad (51)$$

where $A_O = .372$ for human muscle (Hatze, 1981, p. 62). For slow motor units
($n=0$) $m = 3.72$ and for fast motor units ($n=1$) $m = 37.2$. Again an average
value is used for present modelling efforts.

C. Feedback Control

Another property of mammalian skeletal muscles involves the feedback

control between closely related muscles. For example the flexor and extensor

muscles, namely the biceps and triceps, determine in unison the degree of

elbow flexion. The afferent neurous, termed Ia, pass information from the

sensory receptors (usually muscle spindles) in the muscle to the spinal cord

where they form monosynaptic excitatory connections with large α motoneurons

which carry information back from the spinal cord to muscle fibers. Thus

stretch of one muscle will cause excitatory impulses in the spindle to excite

the Ia fiber which in turn exites the α-efferent motoneurons resulting in a

reflex contraction. This monosynaptic reflex arc, shown in Fig. 11a, is known

as stretch reflex. However, in most cases, a voluntary active response will

completely override in magnitude the stretch reflex. Therefore the stretch

reflex hasn't been specifically included in the ATB Model.

A second reflex, termed reciprocal inhibition, involves the collaterals

of the Ia fibers forming disynaptic inhibitory connections with the

antagonistic motoneurons. Activity in the Ia fibers results in excitation of

one set of motoneurons (agonists) and at the same time inhibition of the

antagonistic motoneurons as shown in Fig. 11b. Thus the reciprocal

antagonistic inhibition facilitates contraction of the agonistic muscle

triggered by the Ia fiber activity by simultaneously inhibiting the

antogonistic muscle acting on the same joint (Houk and Henneman, 1967;

Schmidt, 1975; Granit and Pompeiano, 1979). Typically this inhibition appears

to be fairly complete (Granit, 1970) and thus a reasonable assumption is to

eliminate the antagonist muscles completely in voluntary motion involving

reciprocal inhibition.

It is also possible to influence the output of the muscle spindle

afferents and thus adjust the amount of α-efferent activity returning to cause

muscle contraction, by a second set of efferent nerves. These are smaller in

size termed γ, and innervate the intrafusal fibers of the muscle spindle.

Increased γ activity causes an increased timing frequency of the Ia fibers

resulting in increased agonist contraction. Such changes represent a change

in the gain of the system and are included inherently in the motor unit

recruitment algorithm.

Apart from the muscle-spindle receptors, the skeletal muscle contains

another type of receptor, the Golgi tendon organ, that is important for a

27
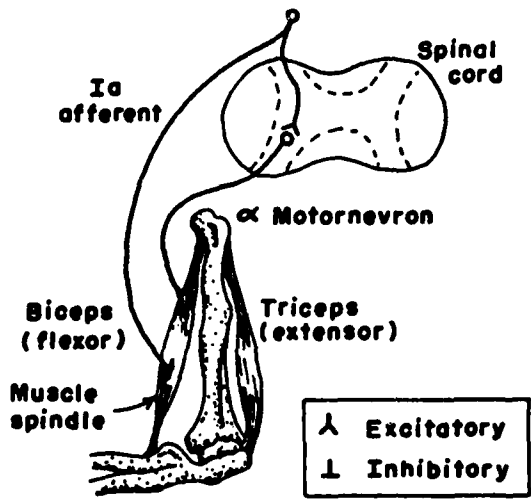
a. STRETCH REFLEX
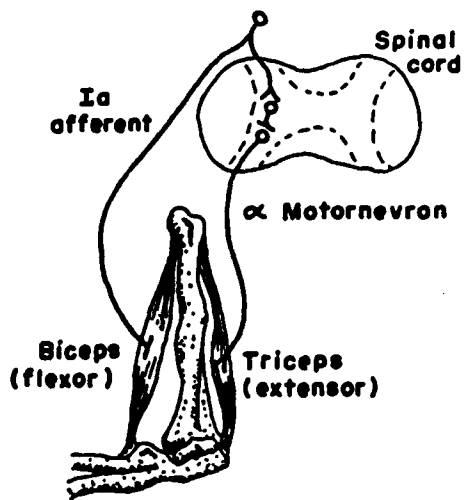
b. RECIPROCAL INHIBITION
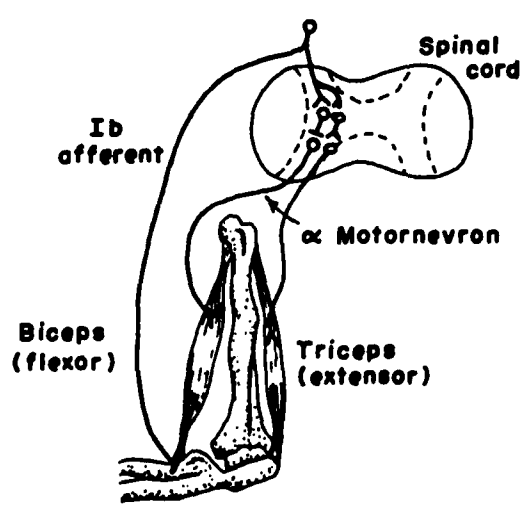
c. CLASP-KNIFE REFLEX
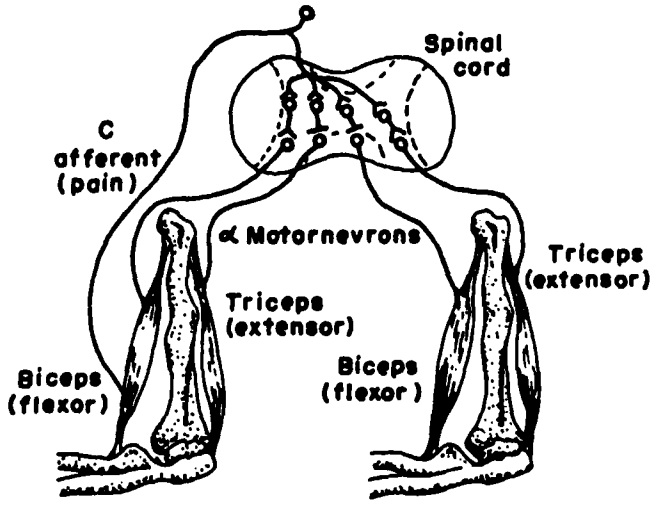
d. FLEXOR AND CROSSED
EXTENSOR REFLEX

Fig. 11   Four Types of Feedback Control

third type of reflex. The Golgi tendon organs are located at the tendons

the extrafusal muscle fibers with afferents termed Ib fibers leading to the

spinal cord. During a muscle contraction the firing frequency of Ib fibers

increases indicating the Golgi tendon organs respond to tension. In

functional terms the segmental connections of the a Ib fibers mirror those of

the Ia fibers. The tendon organs form inhibitory connections with agonistic

motoneurons and excitatory connections with antagonistic motoneurons as shown

in Fig. 11c. A strong increase in muscle tension, whether caused by passive

stretch or active contraction, will lead to inhibition of the agonist

motoneurons via Ib fibers and thus prevent a too strong rise in tension.

Under severe muscle stretch, muscle tone will decline suddenly, resulting in

the clasp-knife reflex which acts to protect the muscle, (Houk and

Hermeman,1962). The first response, is inherently included in the motor unit

recruitment algorithm while the clasp knife reflex is modeled to reduce the

muscle force to zero should the rise be greater than 50 FMAX/sec. This value

is based on maximum speed of motor unit recruitment, ie. FMAX in 100 msec

(Desmedt and Godaux, 1977, 1978). The limiting value of force as t approaches

100 msec (or n approaches 1) is 50 F_{MAX}/sec.

D. Time Varying Effects

The most important time varying effect in the muscle is fatigue. It is

obvious that people can maintain their maximum effort very briefly (5

seconds), whereas they can maintain a force of around a quarter of their

maximum strength for an extended period of time. Such an endurance responses

can be explained by examining the properties of individual motor units. Type

I motor units tend to be more aerobic, less fatigable and are recruited at

lower tension levels. While Type II motor units tend to be an aerobic, more

fatigable and are recruited at higher tension levels, (Stephens and Usherwood,

29

1977). Although exact fatigue and recovery patterns for individual motor units have not been identified, the maximum endurance time can be estimated from experimental studies. The earliest experiments of Miller (1932) implied that the length of time a force could be maintained depended on the fraction of available strength to be exerted. This relationship was further verified by Rohmert, 1960, Kogi and Hakamada, 1962; Caldwell 1963, 1964; Monod and Scherrer, 1965; Schutz, 1972. Only three studies attempted to derive and publish formulas of this relationship. Monod and Scherrer (1965) proposed:

$$T_{END} (min) = \frac{2.5}{((\%F_{MAX}-14)/100)^{2.4}}$$ (52)

Kogi and Hakamada (1962) suggested

$$T_{END}(min) = \frac{5012}{(\%F_{MAX})^{1.99}}$$ (53)

while Schutz (1972) indicated:

$$T_{END}(min) = -1.25 + \frac{125.}{\%F_{MAX}}$$ (54)

All of these formulas have some faults that limit their usefulness in representing the empirical data. Equation 52 does not account well for the asymptotic relationship of endurance approaching indefinite times for force levels of 15-20% MVC. Equations 53 and 54 provide the asymptote but predict

lower than normal endurance times for large force levels. A separate formula was developed for the current work, based on the data of Rohmert (1960), who, with over 300 subjects tested, had the largest sample size. Best fit was produced by the hyperbolic relationship (shown in Figure 12):

$$T_{END}(sec) = \frac{1236.5}{(\%F_{MAX}-15)^{.618}} - 72.5 \tag{55}$$

Once the endurance time is exceeded, however, the person's strength does not immediately fall to zero. For maximal or large submaximal efforts, there is still a gradual decay to the lower level of 15-20 percent found for indefinite holds (Petrofsky, 1982, p. 55). This experimental data can be modelled very easily using polynomial regression with time in minutes:

$$\%F = 98.1 -23.9t + 1.9t^2 \tag{56}$$

V. PHASE III - MODELLING THE GENERAL MUSCULATURE

The attachment of the complete muscle systems to limb segments, includes the identification of joint biomechanics, the measurement of origin and insertion coordinates, the integration of agonist and antagonist actions and computation of cross-sectional areas for estimation of total force production. Methods to accomplish this can be best described according to the joints or area of the body involved.

A. Elbow Joint:

Modelling of the elbow and simulation of elbow flexion is perhaps the easiest case to examine and will serve as a simple example demonstrating the validity of the technique used for the more complicated joints. The model

31

Fig. 12 ENDURANCE TIME AS A FUNCTION OF RELATIVE STRENGTH

32
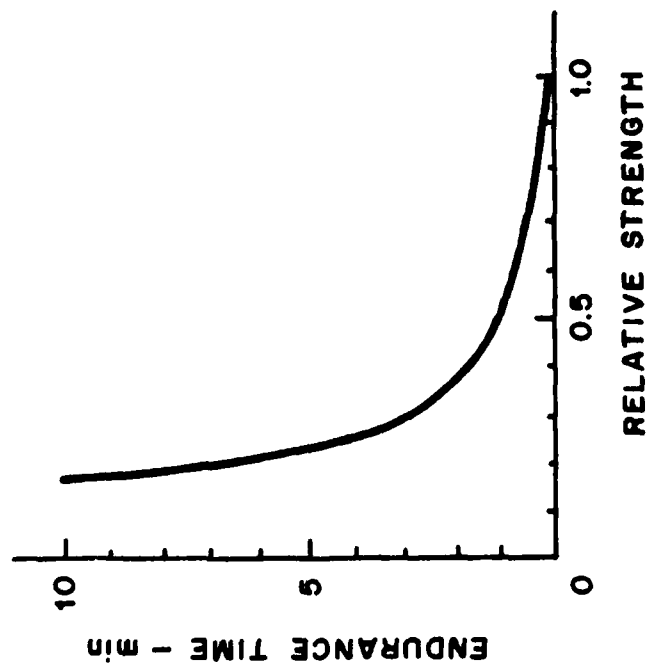
includes two segments: the humerus, and a combination of the ulna and the radius and three elbow flexor muscles: biceps brachii, brachialis and brachioradialis. Examination of the biceps brachii more closely shows the origin of the long head to be at or beyond the gleno - humeral joint (Mc Minn and Hutchings, 1977). The insertion can be set at approximately 3.5 cm from the elbow joint corresponding to the data of Wilkie (1950). Using the cross-sectional area of 4.58 cm^2 for the biceps (Schumacher and Wolff, 1966) and multiplying by the maximum muscle force of 100N/cm^2 (Hatze, 1981) yields a maximum isometric tension of 458 N. (The difference between anatomic and physiological areas due to fiber- orientation are accounted for). Adding the force of 690N generated by the brachialis (6.9 cm^2 x 100 N/cm^2) to the biceps yields a maximum elbow flexion force of 1148 N. Such a value can be compared to the data of Wilkie (1950) who found that his subjects could maintain a maximum force of 195.8 N at the wrist. With a lever ratio between muscle insertion distance and the moment arm of the weight of .15, the maximum elbow flexion force is 1305 N. These values are remarkably close considering that other minor muscles producing additional torque are not accounted for in the first calculation. Similar calculations were conducted on the other muscles.

Complete details on all of the elbow muscles are based on previously collected data (Chao and Morrey, 1978; Youm, et.al. 1979; Maton, et.al. 1980; Amis, et.al., 1980; Hatze, 1981) and are summarized in Table 1, Appendix A.

B. Shoulder Joint:

The shoulder is a much more complicated joint consisting of three separate joints: the glenohumeral joint, the acromioclavicular joint and the sternoclavicular joint. Correspondingly, many more muscles are involved to produce many different actions. Details on the actions of these muscles, points of origin and insertion, along with cross-sectional areas are taken

33

from previous biomechanical studies (Schumacher and Wolff, 1966; Dempster, 1965; DeLuca and Forrest, 1973; Engin, 1980) and given in Table 2, Appendix A.

C. Hip Joint and Knee Joint:

Although consisting of only one joint, the hip is a ball and socket joint and along with the many muscles involved, undergoes many different types of actions. A further complication is that a majority of these muscles span both hip and knee joints and thus hip actions cannot be uniquely separated form knee actions. Details on the actions of these muscles, points of origin and insertion, along with the cross-sectional areas were taken from earlier biomechanical studies (Merchant, 1965; Schumacher and Wolff, 1966; Seireg and Arvikar, 1973; Jensen and Davy, 1975; Crowninshield, et.al. 1978; Dostal and Andrews, 1981; Smidt, 1973; Nissan, 1980; Wismanis, 1980; Minns, 1980) and are summarized in Table 3, Appendix A.

D. Trunk and Neck Musculature:

Simulation of the trunk musculature is a much more difficult undertaking than for the previous joints. First of all, there are many muscles involved, close to 20 major ones for the lower back and trunk and equally many for the neck region. Secondly, some of the muscles, such as the longus, spinalis and semispinalis, have many attachment sites between the different vertebrae. Thirdly, the lines of action of the muscle forces are not always in straight line, e.g., the interior and exterior obliques. Fourthly, the vertebral joints are complicated by the ligaments and their additional force-bearing capabilities. Appropriate approximations were used when necessary.

Details on insertions and origins were obtained from Rab et.al. (1977), Rab (1979), Takashima, et.al. (1979), and Williams and Belytschko (1981), while cross-sectional areas were used from Schumacher and Wolff (1966) and Williams

34

and Belytschko (1981). A summary of these findings is given in Tables 4 (neck) and 5(trunk), Appendix A.

VI. PHASE IV - SOFTWARE IMPLEMENTATION OF ACTIVE ELEMENTS INTO THE ATB MODEL

The software modifications necessary to implement the active elements into the ATB Model are summarized below. The modifications are organized into two sections: 1) changes necesary to increase the number of available muscles (belts within harnesses), 2) changes necessary to model the active elements within a muscle.

A. INCREASING THE NUMBER OF MUSCLES

As described in a previous study (Freivalds, 1982) the incorporation of an active neuromusculature into the ATB model was possible through the use of the advanced restraint system developed by Butler and Fleck (1980). A harness consists of one or more belts, where each belt is defined as a set of straight line segments connecting reference points. These points can be placed within the body simulating a muscle. Unfortunately one of the limitations of the advanced restraint system was that, since being designed as an external harness system, a maximum of five harnesses could be specified. This for modelling the human musculature was an extreme limitation as was demonstrated by Freivalds (1982). Thus one of the primary objectives was to increase the number of available muscles. This was accomplished by increasing the sizes of several arrays and changing related code necessary to handle these arrays.

The arrays necessary for the harness/belt systems are found primarily in common block HRNESS. The following arrays were increased in size from 20 to 50:

XLONG (50) - initial slacks for each belt

35

NPSTPB (50) - number of points per belt

NPTPLY (50) - number of points in play per belt

NTHRNS (50) - index to NTAB array defining the force deflection

functions for each belt.

Array NBLTPH (number of belts per harness) was increased in size from 5 to 50.

In common block forces array BSF (4,20) was changed to BSF (4,50) to

accommodate the increase in the number of belts.

Using a maximum of 50 muscles (harnesses) limits the number of muscle

sections (belts) to one per harness. Reducing the number of muscles

(harnesses) still allows several muscles(belts) per harness. Similarly the

total number of reference points and points in play for all muscles is limited

to 100 (ie. 2 per each muscle for 50 muscles or more if the number of muscles

is reduced).

In addition to increasing the sizes of the arrays directly related to the

harness/belt system, two other arrays NTAB and TAB in the common block TABLES

were also expanded. NTAB contains the index pointers to the TAB array for

each function at the allowed contact points and was expanded from 500 to 1250.

TAB contains function defintions and update information for each contact point

and was expanded from 2600 to 6000. Correspondingly any reference to variable

MXNTB, the number of elements in the NTAB array, and MXNTB2 the total number

of elements in the TAB array, had to be checked. Consequently in subroutine

FDINIT, the following lines were altered:

Line # 51   IF (MXTB2.GT.5000) WRITE (6.62) MXTB2)

Line #54   IF (MXNTB.GT.1250) WRITE (6.63) MXNTB

Line #52   IF (MXTB2.GT.5000 OR MXNTB.GT.1250) STOP 16

Cases of the above arrays being initialized or set equivalent to

36

other arrays were also checked. Thus in subroutine OUTPUT in order to
initialize the arrays in common block FORCES, the limit on the counter in the
DO loop in line #44 must be increased from 760 to 880:

Line #44   DO 11 I = 1,880

In subroutine RSTART, new values of variables to be input are set
equivalent to labelled common blocks. Thus the following lines were altered.

Line #76   DIMENSION RC11 (880), IC11 (9)

Line #93   DIMENSION IC14 (1304)

Line #139   DIMENSION RC23 (1952), IC23 (1050)

In subroutine SEARCH called by subroutine RSTART to compute the labelled
common block numbers and items, corresponding changes again had to be made.
Thus the following lines were altered to become:

Line #7 DIMENSION BVAR (260),KOUNT (25), NDIM (3,260), NJ(3), NK(3),

             INDEX(3)

Line #30   DIMENSION C23(15), NC23(45)

Line #55   EQUIVALENCE (C23(1), BVAR(241)), (NC23(1), NDIM(1,241)).

Line #56   EQUIVALENCE (C24(1), BVAR (253)), (NC24(1), NDIM(1,253))

Line #58   DATA NVAR/260/,KOM/24/, BLANK/8H   /

Line #152   DATA NC11/7,300, 4, 50, 0, 10, 20, 0, 3, 20, 0, 7, 30, 0,

Line #176   1250, 0, 0, 6000, 0, 0/

Line #240   add, 8H FSCALE   , 8H FTYP1   , 8H FMU   /

Line #242   2, 0, 0, 5, 100, 0, 50, 0, 0, 50, 0, 0,

Line #243   50, 0, 0, 50, 0, 0, 50, 0, 0, 50, 0, 0, 50, 0, 0/

To correct for the additional output arising from a large number of
muscle/harnesses, one additional modification may be needed. Should the user
desire tabular time histories of the various events. NPRT (4) on input an A5.

37

must be set according to the specifications in the User's Manual (Fleck and Butler, 1982). The Tabular time histories can be of two types: 1) optional output controlled by input Cards H.1 to H,7 and 2) automatic output. The optional tabular time histories are as follows:

1a) linear accelerations for specified points

1b) linear velocities for specified points

1c) linear displacements for specified points

1d) angular accelerations for specified points

1e) angular velocities for specified points

1f) angular rotations for specified points

1g) joint torques

The automatic tabular time histories are as follows:

2a) plane-segment contacts

2b) belt-segment contacts

2c) muscle-harness forces

2d) spring damper forces

2e) segment-segment contacts

2f) airbag-segment contacts

During program execution the above calculated values are stored in the array ZTTH in common block TMPVS by subroutine POSTPR and printed by subroutine HEDING. In the present version, array ZTTH was dimensioned (14,45,2) allowing theoretically approximately 7 tabular time histories. However, since the common block TEMPVS was dimensioned to a larger size in the main program array, ZTTH overran its normal boundaries but stayed within the size of the total common block TEMPVS which is equal to 10538 integer words By default this allowed approximately 38 tabular time histories. With an

38

increased number of muscle/harness systems and corresponding automatic tabular

time histories there is much greater chance to overflow common block TEMPUS

and crash the program. Thus array JTMPVS in common block TEMPVS in the main

program was increased from 10538 to 40,000 integer words. (Each integer word

is equal to four bytes). This should allow approximately 200 tabular time

histories which should be sufficient for 50 muscle/harness systems and a

variety of other segment-plane-airbag interactions. In case there is a

problem with array size limitations and overflow, the dimension of array

JTMPVS can be increased according to the number of points or contacts

specified in 1a)-1g) and 2a)-2f) above. Thus

OPTIONAL (#1a+#1b+#1c+#1d+1e+1f) X 4 + (#1g) X 7

AUTOMATIC = (#2a) X 7 + (#2b + #2c + #2d) X 4 + (#2e) x10 + (#2f) x 3

INTEGER WORDS FOR JTMPVS = (#OPTIONAL + #AUTOMATIC) X 45 + 3560

B. ACTIVE NEUROMUSCULATURE

As described previously in earlier works (Freivalds, 1982; Freivalds,

1984), the incorporation of active muscle elements was accomplished through

the use of the advanced restraint system developed by Butler and Fleck

(1980).

In the present effort, instead of merely manipulating input data and

using the existing software to simulate an active neuromusculature, an

additional subroutine named MUSCLE, was written and incorporated into the ATB

Model. Subroutine MUSCLE, however, still maintains the basic or

organizational relationships of the active restraint system, but only

specifies more accurately active muscle parameters. This modification is

transparent to the user allowing the flexibility of using old input data

without musculature as well as new input data with musculature on the same

software.

39

The modifications needed to incorporate an active neuromusculature in the present ATB Model can be summarized as follows:

1) A new subroutine named MUSCLE was written and incorporated into the code

2) Major changes occurred in subroutine HINPUT

3) Minor changes occurred in subroutines FDINIT and HBELT.

These modifications will be described in detail in the following sections.

1. Subroutine MUSCLE

The complete code for subroutine MUSCLE is given in Appendix B and a flowchart of the logic is given in Fig. 13. The basic logic is as follows. Upon entry to subroutine MUSCLE the current time is adjusted by the delay time which is specified by the user in subroutine HINPUT. Thus the user can insert a 10-30 msec delay to account for nerve conduction times, a 150-200 msec delay to account for reaction times, or even longer delays depending on the circumstances. Irregardless of the delay time, the passive (spring and viscous damping) muscle forces are calculated continuously. The active muscle forces are calculated only when the current time exceeds the delay time.

Next the percent of motor units (% mu) recruited for that given time is calculated. The rate of recruitment is specified by the user in subrouting HINPUT. This rate can vary from a maximum rate of 100% mu recruited (or maximum force) in 100 msec to much slower rates in seconds. The program checks that this maximum rate, based on the ballistic muscle contraction data collected by Desmedt and Godaux (1977, 1978), is not exceeded.

Next the program compares the % mu recruited with the percent of Type I mu as specified by the user (in subroutine HINPUT). If the % mu recruited is less than the % of Type I mu then contraction times based on Type I mu

40
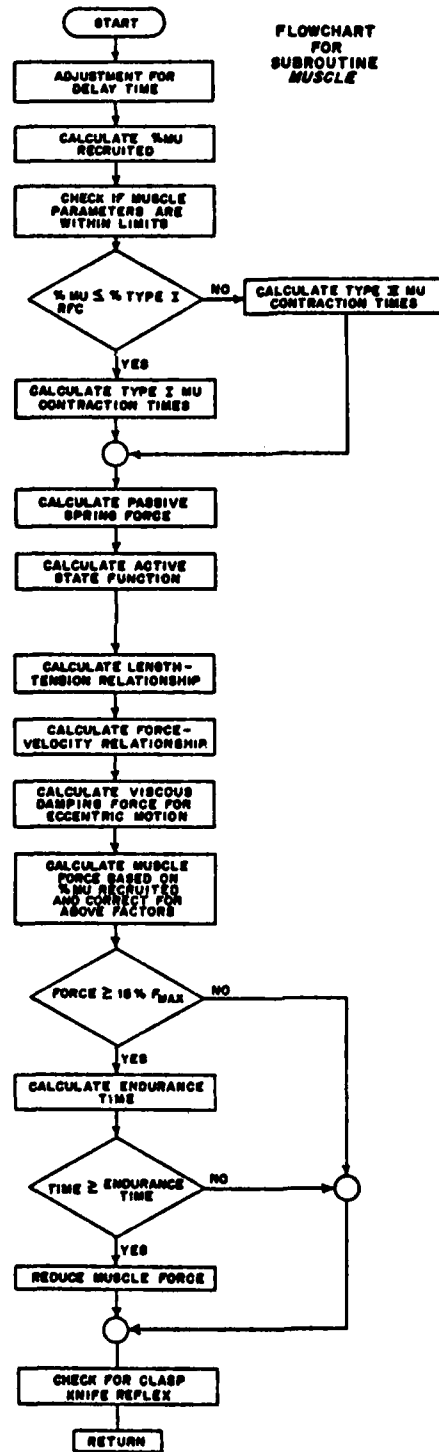
Fig. 13 Flowchart of Subroutine MUSCLE

41

properties are calculated. If the % mu recruited exceeds the % of Type I mu, then contraction times based on Type II mu properties are used. Next the fractional forces developed by the various elements as described in Chapter I are calculated. The total muscle force based on % mu recruited is then calculated and adjusted by the fractions contributed by each element. Finally an endurance time based on the total muscle force is calculated. If the current time is less than the endurance time, the muscle force remains unaltered. However, if the current time is greater than the endurance time the muscle force is reduced proportionately according to Eq. 56.

2. Subroutine HINPUT

The complete code for subroutine HINPUT is given in Appendix C. The major changes are involved in supplying additional muscle parameters on the F.8.C card. These changes occur between lines 53-57 in subroutine HINPUT. The primary input in line #53 becomes,

READ (5, 14) NF, XLONG (J),FSCALE(J) FTYP1(J), FMU(J), RECTIM(J), DEL(J).

Where FSCALE(J) = Scaling factor for maximum muscle force

FTYP1(J) = percent Type I motor units (range: 0-100)

FMU(J) = percent motor units recruited (range: 0-100)

RECTIM(J) = Motor unit recruitment time (seconds)

DEL(J) = delay time before motor unit recruitment (seconds)

and the format in line #54 becomes:

14 FORMAT (5I4, F12.0, 5F8.0)

Thus the format and order for the previous input variables remains the same and the additions become transparent to a user not concerned with them. Since the E card functions, previously used to define the muscle characteristics, are not needed, these can be left blank or zeroed. However NF(1) must be specified with a negative value to indicate that a muscle and not a harness is

42

being defined. Since the previous version allowed only NF(2), NF(3) and NF(4) negative for rate dependent functions, but not NF(1), these become mutually exclusive definitions.

Then depending on the value of NF(1), two different echos are produced. If NF(1) $\geq$ 0 the previous format in line #55 is left unaltered:

IF (NF(1).GE.0) WRITE (6,15) I,J,NF,XLONG(J),UNITL

whereas for the current version and NF(1) $\leq$ 0 the following is inserted:

IF (NF(1).LT.0) WRITE (6,19) I, J,FSCALE (J), UNITM, FTYP1(J), FMU(J), RECTIM(J), DEL(J)

with its apropriate format statement. Also, several statements are inserted to check whether the input parameters are within limits.

1) The percent of Type 1 mu must be less than 100:

IF (FTYP1(J).GE. 100.) FTYP1(J) = 99.99

2) The percent of Type 1 mu must be greater than or equal to zero.

IF (FTYP1(J).LE.0) FTYP1(J) = .0001

3) The first 30% of mu recruited must be Type I.

IF (FMU(J).LE.30. .AND. FMU(J).GT.FTYP1(J)) FTYP1(J) = FMU(J)

4) Finally two statements change percent values to fractional values.

FTYP1(J) = FTYP1(J)/100.

FMU(J) = FMU(J)/100.

Revised instruactions for defining the F.8. cards are given in Appendix D.

3. Minor Modifications

In subroutine HBELT at line#84, depending on the value of the first harness function, ie. NF(1), either the new subroutine MUSCLE or the old subroutine FRCDFL is called to calculate the forces due to strain and strain rate thus:

NM = NTAB (NT+1)

```
IF (NM.LT.0) CALL MUSCLE (etc)

IF (NM.GE.0) CALL FRCDFL (etc)
```

Also Line #78 was eliminated to allow for negative stains, which is necessary for concentric muscle motion.

In subroutine FDINIT, to eliminate the need of storing E-card functions not required for the active musculature, three lines were inserted after line #21:

```
IF (NF(1).GT.0) GO TO 50

NTAB(NT) = -1

GO TO 56
```

and line #22 was given line number 50.

VII. SIMULATION AND VALIDATION

A. SIMULATIONS OF TRUNK AND NECK MUSCULATURE

In Phase IV, the advanced neuromuscular model was validated via simulation of human body responses to high G(lateral) acceleration. Data obtained under similar conditions on air crew personnel experiencing tests in the Dynamic Enviornmental Simualtor at Wright-Patterson AFB, OH, were used for comparison purposes. Some of this data was used in an earlier pilot study developing a trunk musculature (Freivalds, 1984).

The full ATB Model with 15 body segments (head, neck, upper torso, center torso, pelvis, upper arms, lower arms, upper legs, lower legs, and feet) and 14 joints (head junction, neck junction, waist, L_5/S_1, joint, two hips, two knees two ankles, two shoulders, two elbows) was utilized to provide an adequate human neuromusculature. The muscles described in Chapter V and summarized in Tables 1-5 needed to be added to the existing ATB Model. For each muscle specific coordinates of origin and insertion points were determined form anatomical texts

44

(Quiring et.al., 1945; Quiring, 1947; Gray, 1974; McMinn and Hutchings, 1977).

Cross sectional areas obtained from Schumacher and Wolff (1966) and Williams and

Belytschlso (1981) were multiplied by the muscular force constant of 100 N/cm^2

(Hatze,1981) to determine a muscle force scaling factor. These resulting values

were then converted to English units for use in the present ATB Model mode and

are summarized in Tables 6-10, Appendix E.

For the simulations of responses to lateral G forces, the body segments

were arranged in the semi-reclining posture maintained by air crew personnel in

the cockpit. The lower trunk was restrained by a lap belt; the feet fixed on

the floor; any other restraints, such as shoulder pads or hands placed on

controls, were eliminated. Only the neck and trunk musculature on the right

side of the body were activated so as to reduce program complexity and execution

times. A 2 Gy lateral force was applied to the body and the acceleration;

velocity and displacement of various body segments were recorded.

A graphical response of the whole body response (using only tr-ink and neck

musculature) to the lateral force over time is shown in Figure 14. For

comparison purposes, the response to a control case with no musculature is given

in Figure 15a, while the response using the previous simplified musculature is

given in Figure 15b. Although the musculature does not completely prevent the

lateral deflection of the body, the response is significantly delayed with head

and neck maintaining the upright position for a longer period of time. The

result is better observed in Figure 16, which shows the plot of angular

displacement of the upper trunk for all three conditions. At the end of 256

msec the angular displacement is reduced by 20° with the use of musculature.

Based on the time history, the response with the musculature lags up to 40 msec

behind the control response.

B. SENSITIVITY OF MUSCLE ORIGINS AND INSERTIONS

45

Fig. 14 — Graphical Display of Trunk Response to Lateral G_Y-Forces (2G)
(Current work)

TIME(MSEC) 96.0   TIME(MSEC) 192.0   TIME(MSEC) 256.0
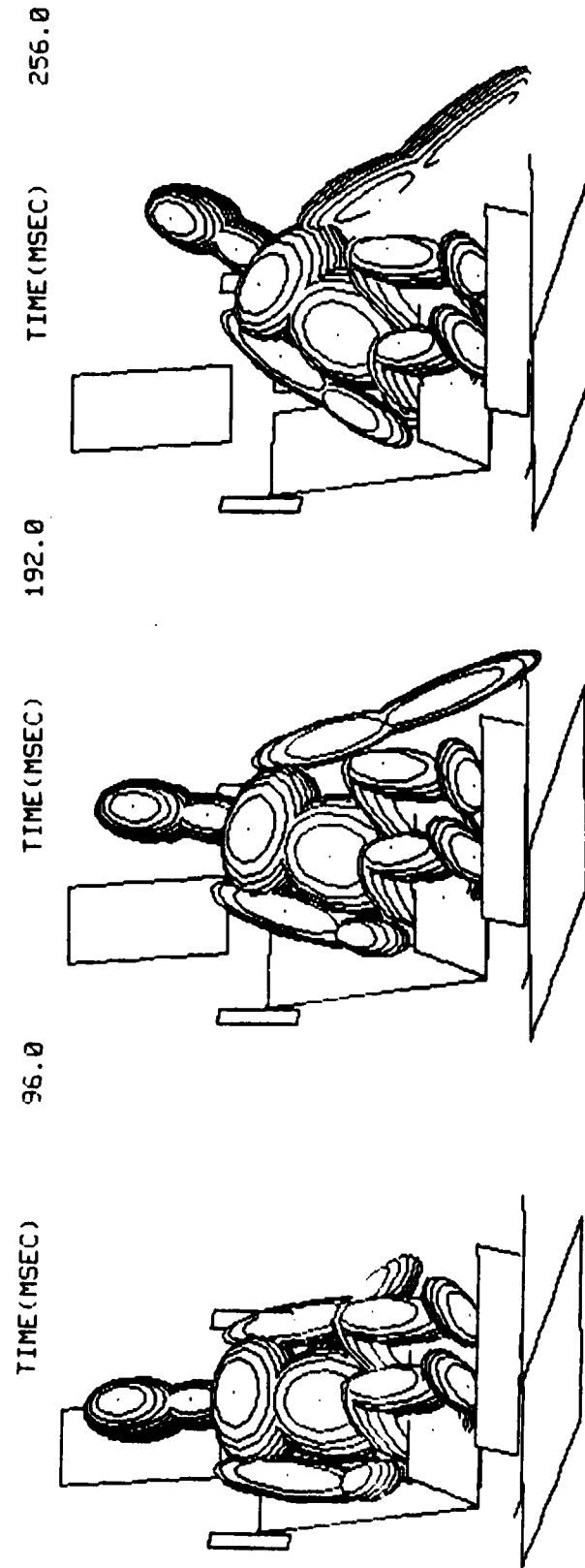
a. Control condition

TIME (MSEC) 96
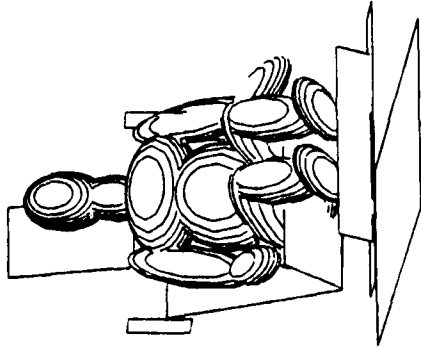
TIME (MSEC) 192
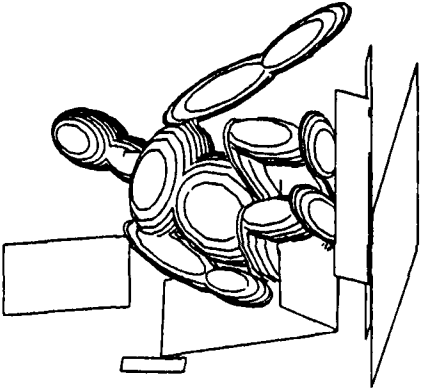
TIME (MSEC) 256
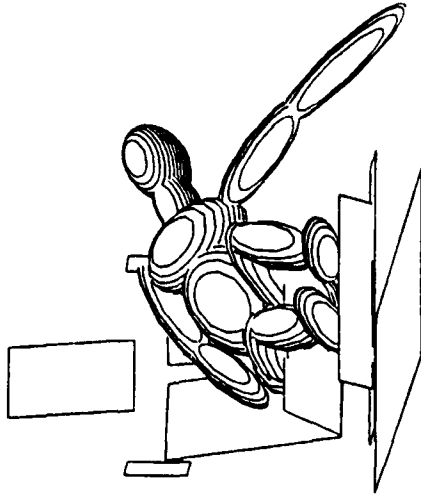
b. Neuromusculature (Freivalds, 1984)

TIME (MSEC) 192
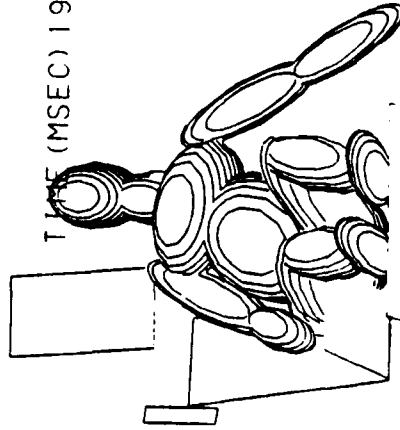
TIME (MSEC) 256
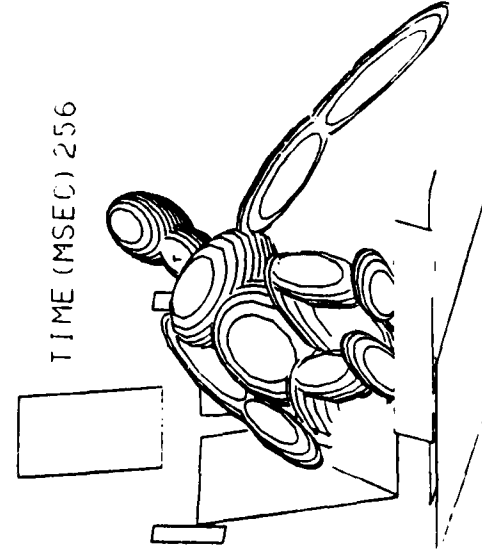
Fig. 15 - Graphical Display of Trunk Response to Lateral G_y Forces (2G)

47

Fig. 16 ANGULAR DISPLACEMENT (ROLL) OF UPPER
TRUNK DUE TO LATERAL G-FORCES

48
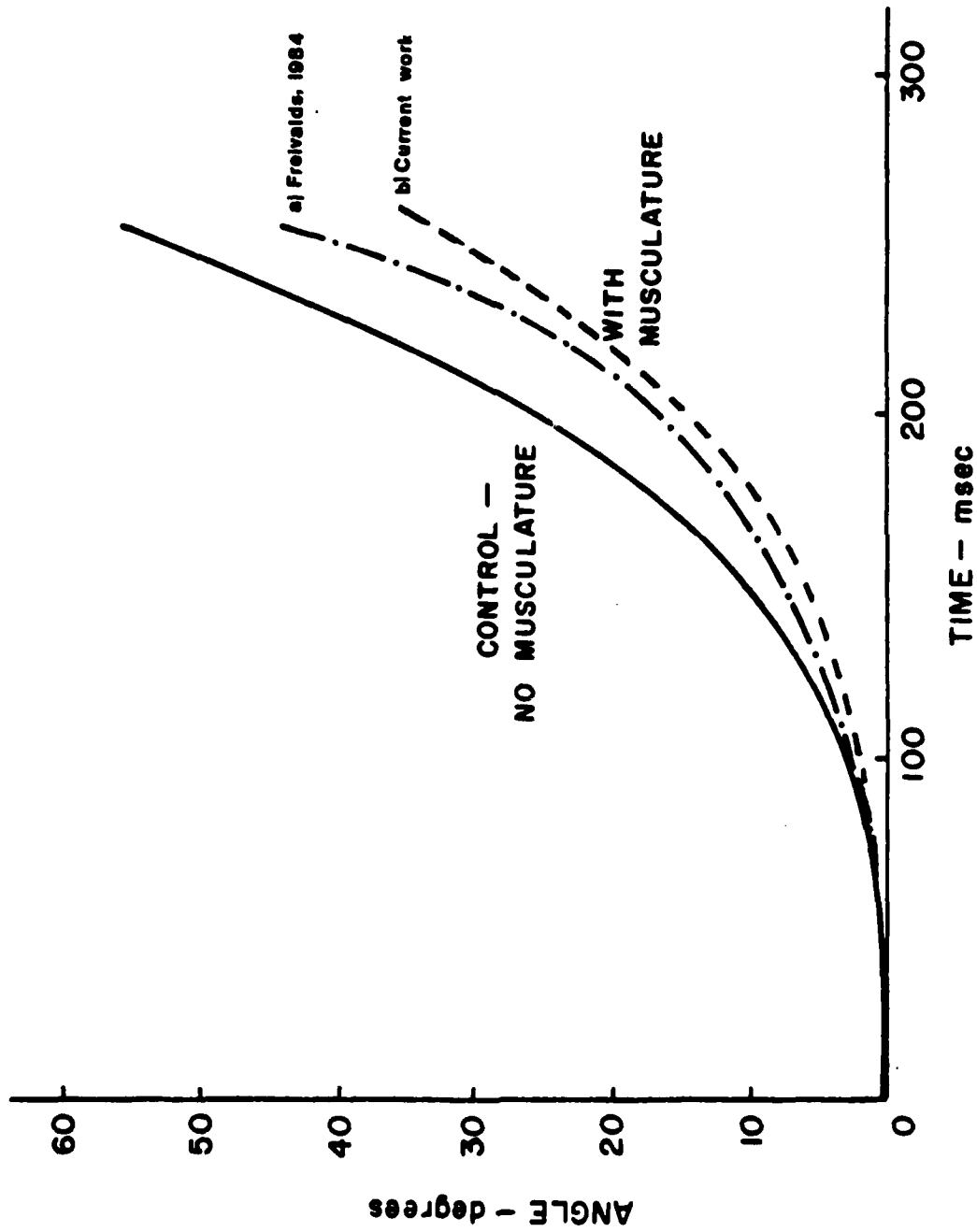
One important factor effecting the accuracy in stimulating the active neuromusculature is the accuracy of the placement of the musculature, i.e. the origins and insertions of the muscles being used. The origins and insertions specified in Appendix E were derived from anatomy texts such as McMinn and Hutchings (1977), typically by measuring directly from scale photographs of the anatomical structures. Obviously, some human error is involved, especially in using two dimensional photographs of three dimensional structures. Thus it was decided to simulate errors in muscle placement and compare the resulting muscle forces with "true" muscle placements.

Five different cases were used in simulating elbow flexion with three muscles: the biceps brachii, the brachialis and the brachioradialis. In Case 1, the origin of each muscle was displaced by 10% of the insertion distance. In Case 3 both origins and insertions were shifted by 10%. In Case 4 both origins and insertions were shifted by 20% of the distance. Case 5 was the control condition with "true" origins and insertions. The simulation was of elbow extension using a weight of 60 lbs. held in the hand as shown in Fig. 17. Since this weight exceeded the maximum weight that could be maintained at 90° of elbow flexion, the muscle were were forcibly extended in an eccentric fashion. The resulting muscle forces were plotted as a function of the included elbow angle in Figs. 18-20.

The general motion of the curves can be best explained by the forces produced by each of the elements involved in the muscle model. The rather sharp overall increase is due to the force velocity relationship for eccentric motion. The damping function also adds some force with increasing speed. But as the arm is extended further, the length tension relationship contributes significantly in reducing the force. The brachioradialis is most affected, the biceps the least. However, for all four cases there is minimal deviation from the norm

49

Fig. 17   ANATOMY OF THE ELBOW FLEXORS
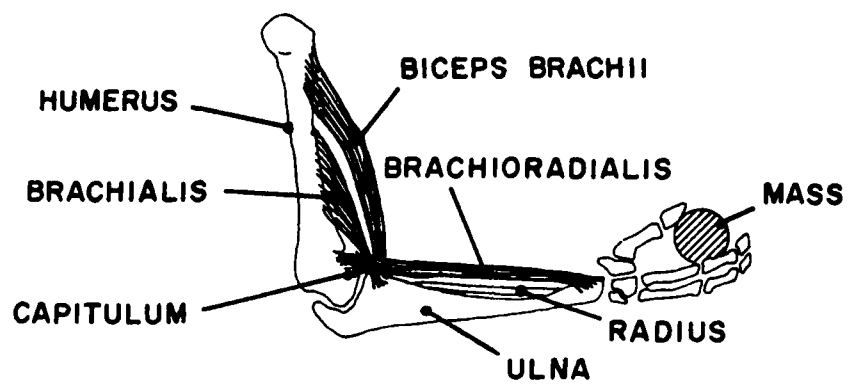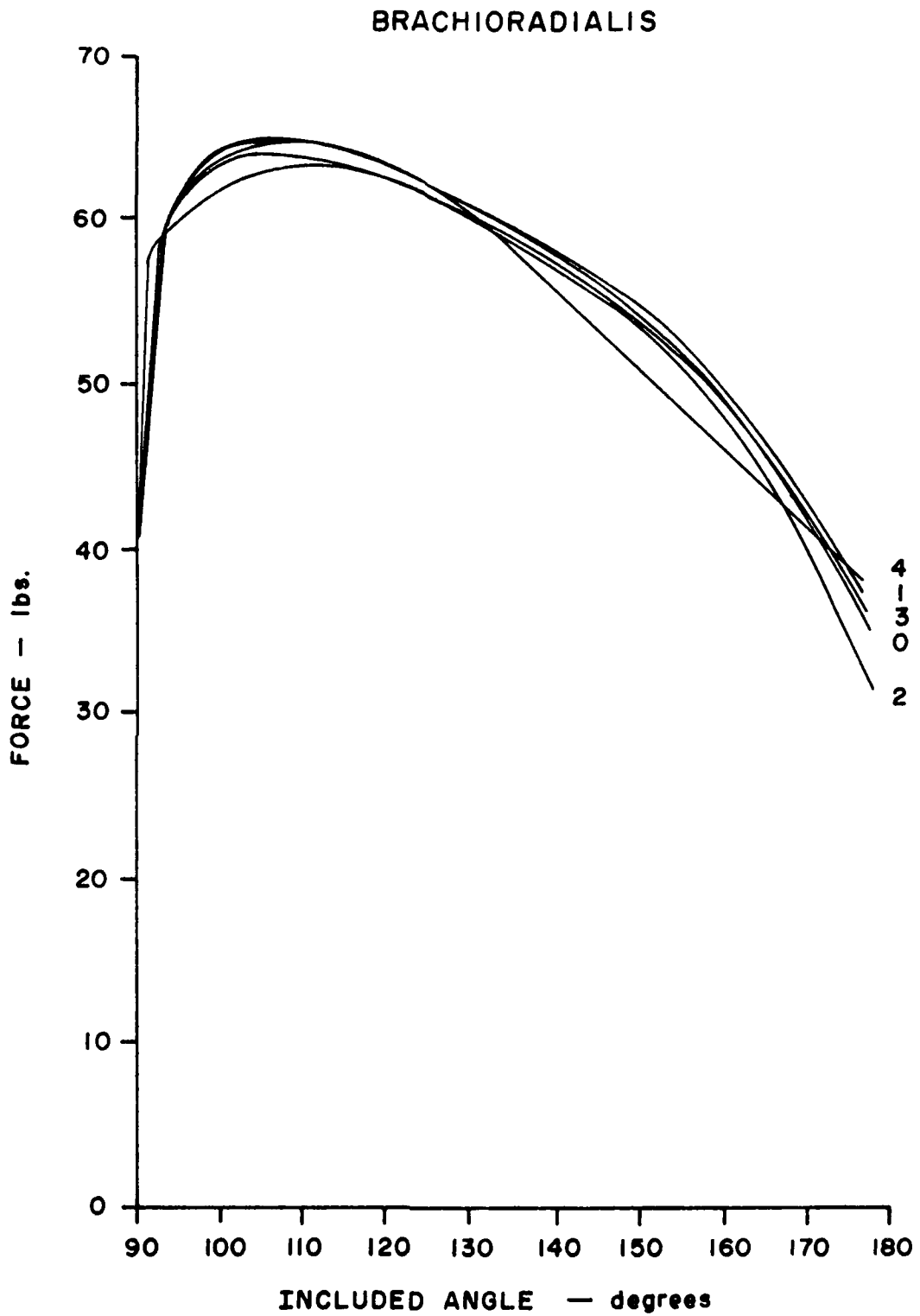
BRACHIORADIALIS

Fig. 18   Force Production by the Brachioradialis during Eccentric
Motion

51
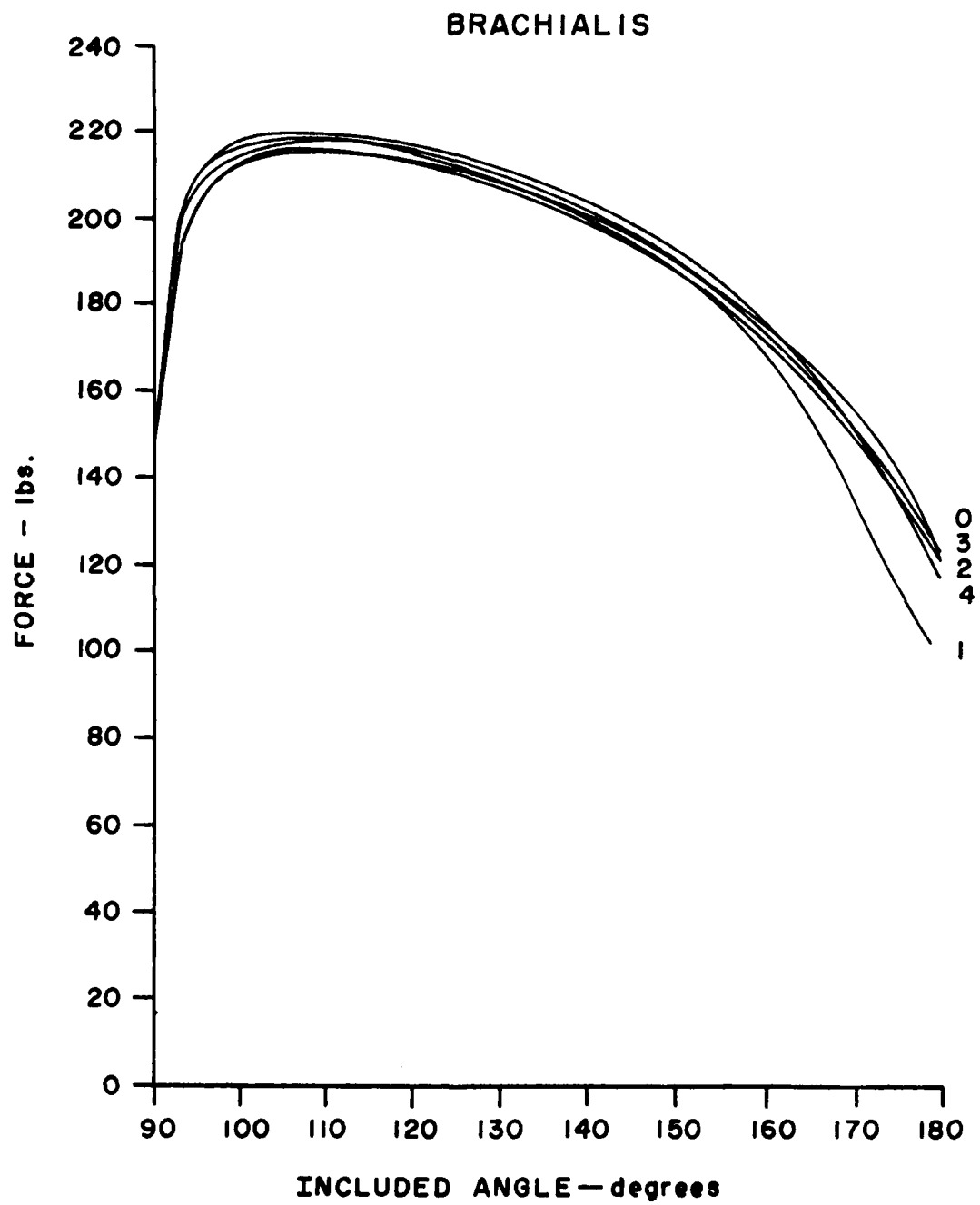
BRACHIALIS

Fig. 19   Force Production by the Brachialis during Eccentric Motion

52

BICEPS BRACHII
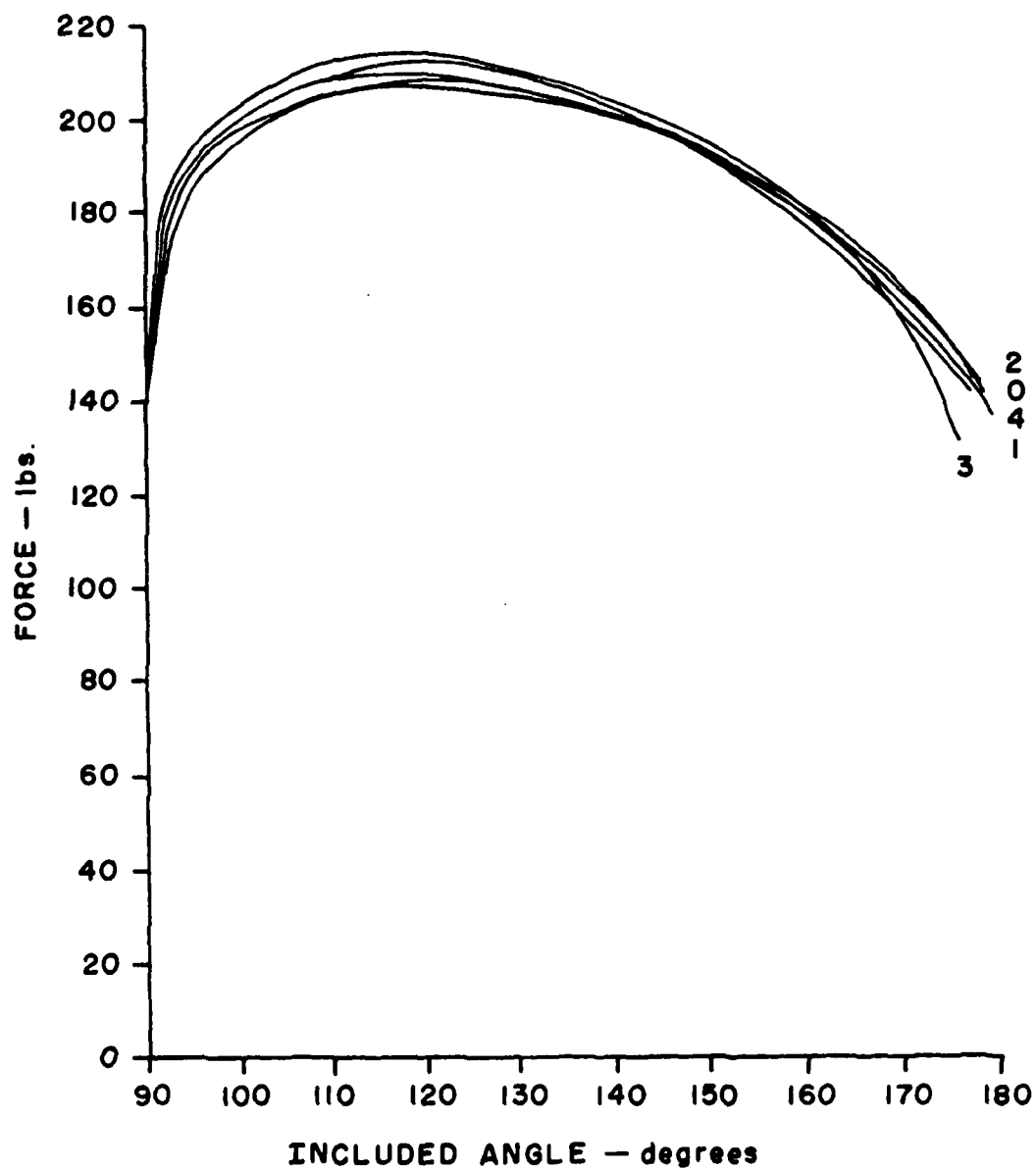
Fig. 20   Force Production by the Biceps during Eccentric Motion

53

with an average deviation of about 3%. The maximum deviation is 9%. Thus for most practical purposes, deviations in muscle origins and insertions will not be significant for eccentric motions.

Concentric muscle contractions, using a weight of 15 lbs., were also simulated. The results are plotted an described in detail in Appendix F. In general, for all the curves, there was a sharp decrease in force due to the force velocity relationships, with a later recovery as the velocity decreased. There were greater deviations from the norm - averging about 5% but reaching up to 10%. Again the brachioradiales showed greatest effect especially for Case 2. This is due to a configuration opposite of the biceps and brachialis, acting more as a shunt rather than a spurt muscle (MacConail, 1949).

Only a slight deviation is noticable for Cases 3 and 4. Perhaps this can be rationalized by having the effects of both offsets cancel each other out.

C. ANATOMICAL STUDIES OF TRUNK MUSCULATURE

Other simulations of trunk musculature were also attempted. Special efforts were applied to generate accurate crossectional areas, as well as muscle origin and insertion points. The details of muscle cross sectional areas as investigated by C. S. Davis are presented in Appendix A.

VIII. CONCLUSIONS

Further simulations of various human body motions or responses to external forces need to be conducted in order to more adequately validate the model. These would include not only additional lateral forces, but also forward/back (Gx) and up/down (Gz) forces as well as multidirectional forces. Various combinations of muscle parameter values need to be tested, so as to determine the optimum values for generating the most realistic human response.

54

Similarly, further examination of other neuromuscular reflexes may still lead to further improvements in the model. However, the simulations demonstrated that the presently developed muscle model can adequately represent an active human neuromusculature response to dynamic mechanical stresses and can serve as a cost effective research and developmental tool.

APPENDIX A

INPUT DATA FOR HUMAN MUSCULATURE
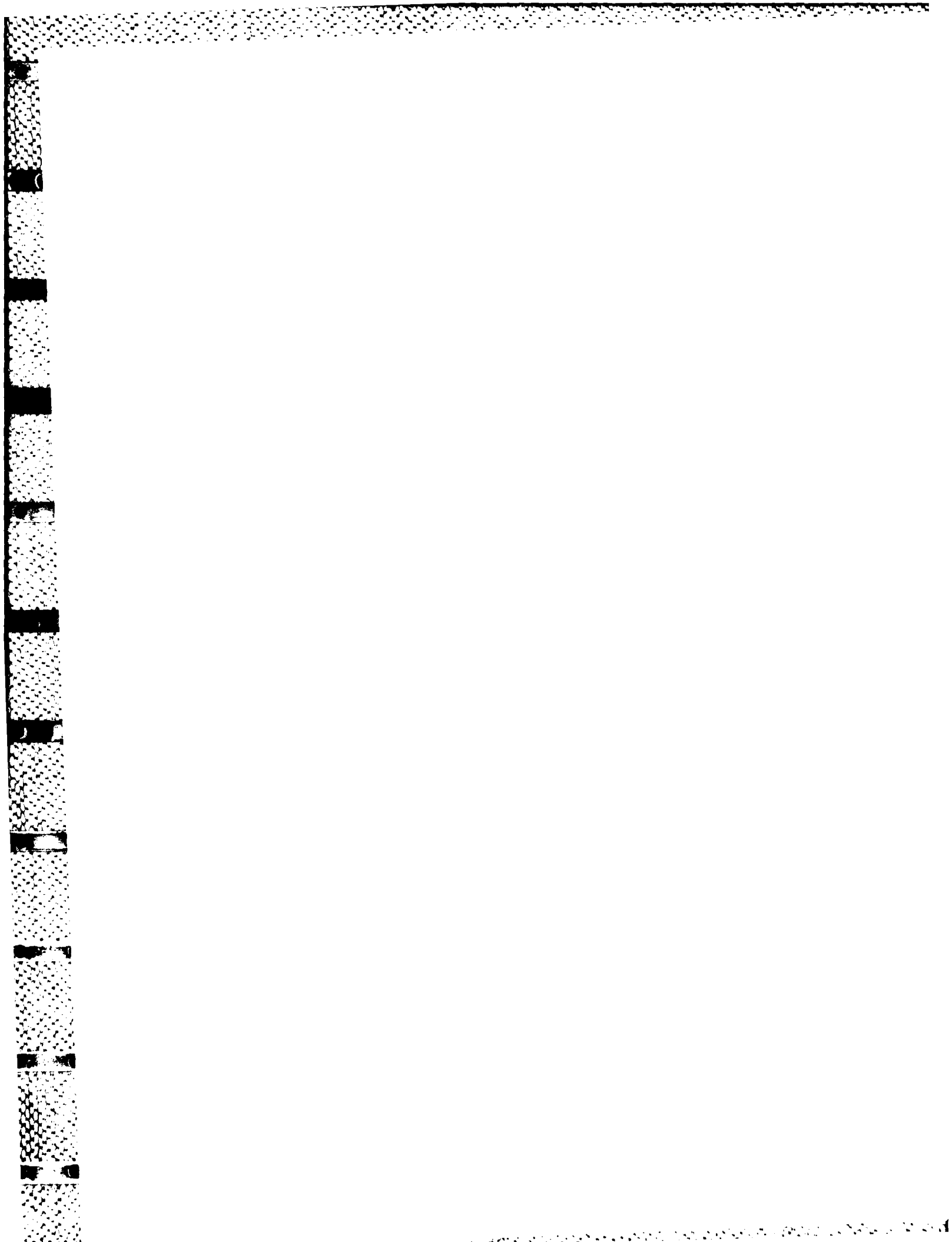
APPENDIX A

INPUT DATA FOR HUMAN MUSCULATURE

Table 1. Specifications on Elbow Musculature

Muscle Group	Origin	Insertion	Action	Cross-Sectional Area (cm2)
Biceps brachii	Short head from coracoid process of scapula, long head from supraglenoid tuberosity	Radial tuberosity	Flexion of forearm	3.55
Brachialis	Lower anterior surface of humerus	Coronoid tuberosity of ulna	Flexion of forearm	4.63
Brachioradialis	Proximal two-thirds of humerus	Styloid process of ulna	Flexion of forearm	1.37
Triceps brachii	Long head from infraglenoid tunerosity of scapula, lateral and medial head from posturior surface of humerus	Olecranon	Extension of forearm	16.38
Anconeus	Lateral epicondyle humerous	Olecranon	Extension of forearm	.94
Pronator teres	Medial epicondyle of humerus	Middle of radius	Pronation of forearm	1.61
Supinator	Lateral epicondyle of humerus	Lateral and anterior surface of radius	Supination of forearm	1.77

A-1

Table 2.   Specifications on Shoulder Musculature

Muscle Group	Origin	Insertion	Action	Cross-Sectional Area (cm^2)
Deltoid	Clavicle, scapula acromion	Deltoid tuberosity of humerus	Abduction of arm	11.01
Supraspinatus	Supraspinous fossa of scapula	Greater tuberosity of humerus	Abduction of arm	3.3
Pectoralis major	Clavicle, Stermum	Bicipital groove of humerus	Adduction of arm	6.8
Latissimus dorsi	Lower Thoracic and lumbar vertebrae	Bicipital groove of humerus	Adduction of arm	5.37
Teres major	Inferior angle of scapula	Bicipital groove of humerus	Adduction of arm	4.97
Teres minor	Axillary border scapula	Greater tuberosity of humerus	Adduction of arm	1.57
Subscapularis	Subscapular fossa scapula	Lesser tuberosity of humerus	Flexion of arm	9.9
Coracobrachialis	Coracoid process scapula	Medial border of humerus	Flexion of arm	1.52
Infraspinatus	Infraspinous fossa of scapula	Greater tuberosity of humerus	Extension of arm	5.98

Table 3 Specifications on Hip and Knee Musculature

Muscle Group	Origin	Insertion	Action	Cross-Sectional Area (cm^2)
Gluteus medius	Iliac crest of pelvis	Greater trochanter of femur	Abduction of thigh	21.18
Gluteus minimus	Outer surface of ilium (pelvis)	Greater trochanter of femur	Abduction of thigh	9.6
Tensor fasiae latae	Anterior part of iliac crest of pelvis	Iliotibial tract of femur	Abduction flexion of thigh	2.48
Obturatus internus	Obturatus foramen area of pelvis	Greater trochanter of femur	Abduction of thigh	3.91
Adductor longus	Pubis of pelvis	Linea aspera of femur	Adduction flexion of thigh	5.03
Adductor brevis	Pubis of pelvis	Below lesser trochanter of femur	Adduction flexion of thigh	4.54
Adductor magnus	Ischial tuberosity of pelvis	Linea aspera of femur	Adduction flexion of thigh	20.58
Pectineus	Pubic tubercle of pelvis	Below lesser trochanter of femur	Adduction flexion of thigh	2.47
Quadratus femoris	Ischial tuberosity of pelvis	Quadrate tubercle of femur	Adduction of thigh	2.91
Obturatus externus	Obturator foramen area of pelvis	Trochanteric fossa of femur	Adduction of thigh	4.95
Gluteus maximus	Iliac crest of sacrum	Iliotibial tract of femur	Extension of thigh	29.42
Semimem-branosus	Ischial tuberosity of pelvis	Upper part of tibia	Extension of thigh flexion of leg	12.97
Semitendi-nosus	Ischial tuberosity of pelvis	Medial condyle tibia	Extension of thigh flexion of leg	4.33

Table 3 (Continued)

Biceps femoris	Ischial tuberosity of pelvis, linea aspera of femur	Lateral condyle of tibia, head of fibula	Extension of thigh, flexion of leg	11.8
Quadriceps femoris	Iliac spine of pelvis anterion surface of femur	Patela	Flexion of thigh extension of leg	56.0
Iliopsoas	L2-L4 vertebral bodies, iliac fossa of pelvis	Lesser trochanter of femur	Flexion of thigh	15.06
Gastrocnemus	Medial and lateral condyles of femur	Calcaneus	Flexion of leg	15.66
Popliteus	Lateral condyle of femur	Posterior surface of tibia	Flexion and rotation of leg	1.99
Gracilis	Pubic symphysis of pelvis	Upper medial surface of tibia	Flexion of leg, adduction of thigh	1.63
Sartorius	Iliac Notch of of pelvis	Upper Medial surface of tibia	Flexion of leg and thigh	1.55

Table 4 Specifications on Neck Musculature

Muscle Group	Origin	Insertion	Action	Cross-Sectional Area (cm^2)
Longus Capitis	Transverse processes of C3, C4, C5, C6	Basilar part of occipital bone	Flexion of head	.75
Rectus capitis anterior	C1 transverse processes	Front of foramen magmum on occipital bone	Flexion and notation of head	.25
Rectus capitis lateralis	C1 transverse processes	Jugular process of occipital bone	Lateral flexion of head	.25
Rectus capitis posterior major	C2 spinous process	Inferior nuchal line of occipital bone	Extension, lateral flexion of head	.50
Rectus capitis posterior minor	C1 spinous process	Inferior nuchal line of occipital bone	Extension, lateral flexion of head	.385
Obliquus capitis superior	C1 transverse processes	Inferior nuchal line of occipital bone	Extension and lateral rotation of head	1.00
Splenius capitis	Spinous process of T1 and C7	Occipital bone and temporal bone	Extension and lateral flexion of head	1.22
Longissimus capitis	Transverse processes of T1, C6, C4	Mastoid process of Temporal bone	Extension and Lateral flexion of head	.5
Spinalis capitis	Transverse processes of T1 and C7	Between superior and inferior nuchal line of occipital bone	Extension and lateral flexion of head	.5
Semispinalis capitis	Transverse processes of T1 and C7	Between superior and inferior nuchal line of occipital bone	Extension and lateral flexion of head	2.38

Table 4 (Continued)

Trapezius	Heads of clavicles and and spines of scapulae	Occipital bone and thoracic vertebrae	Extension lateral flexion of head	10.6
Sternocleidomas-toideus	Head of sternum, medial sections and heads of clavicles	Occipital bone and temporal bone	Lateral flexion and flexion of head	.1.6
Levator scapulae	Medical sections of scapulae	Transverse processes of C1, C3	Lateral flexion of neck	17.75
Longus colli	Anterior side of body of C5 anterior side of body of C6 anterior side of body of T1	Anterior side of body of C4 anterior side of body of C3 anterior side of body of C4	Flexion of neck	.75
Scalenus anterior, medius and posterior	Medial clavicle	C3, C4, C5, C6, C7 transverse processes	Flexion and laterial flexion of neck	1.75
Splenius cervicis	T1 spinous process	Transverse processes of C1, C2 C3	Lateral flexion of neck	.7
Longissimus cervicis	T1 transverse processes	Transverse processes of C2, C3, C4, C5, C6	Extension of neck	.6
Spinalis cervicis	Spinous process of T1 and C7	C2 spinous process	Extension of neck	1.25
Semispinalis cervicis	Transverse processes of T2 and C7	Spinous process of C2, C3, C4 and C5	Extension of neck	2.00

A-6

Table 5 Specifications on Trunk Musculature

Muscle Group	Origin	Insertion	Action	Cross-Sectional Area (cm^2)
Iliocastalis lumborum	Transverse processes L1-L5	Lower six ribs	Extension and lateral flexion of vertebral column	1.0
Iliocostalis dorsi	Lower six ribs	Upper six ribs	Extension and lateral flexion of vertebral column	.5
Longissimus dorsi	Transverse processes L1-L5	Transverse processes T1-T12	Extension and lateral flexion of vertebral column	1.0
Spinalis dorsi	Spinous processes L2, L1, T12, T11	Spinous processes T4-T8	Extension and lateral flexion of vertebral column	1.0
Semispinalis dorsi	Transverse processes T7-T12	Spinous processes C6, C7, T1, T2, T3	Extension and lateral flexion of vertebral column	1.0
Multifidus	Transverse processes C5-T12	Spinous processes above vertebra of origin	Extension and lateral flexion of vertebral column	1.25
Interspinales	Spinous processes L5-C2	Spinous processes above vertebra of origin	Extension of vertebral column	.5
Intertransversarii	Connect adjacent transverse processes		Lateral flexion of vertebral column	.25

Table 5   (Continued)

External Oblique	Anterior half of iliac crest	Lower 8 ribs	Compresses abdomen	6.85
Internal oblique	Anterior half of iliac crest	Lower 3 ribs and mid line of body	Compresses abdomen	5.68
Rectus abdominus	Pubic symphysis	Xyphoid process	Flexes vertebral column	2.66
Quadratus Lumborum	Iliac crest	Transverse processes L1-L4	Flexes vertebral column	2.8

APPENDIX B

LISTING OF FORTRAN IV SOURCE DECK FOR
SUBROUTINE MUSCLE

```
      SUBROUTINE MUSCLE (D,RATE,M,N,F,ELOSS,IM,XTIME)
C                                                       REV 6/30/85
      IMPLICIT REAL*8(A-H,O-Z)
      COMMON/TABLES/MXNTI,MXNTB,MXTB1,MXTB2,NTI(50),ITAB(1250),TAB(6000)
      COMMON/HRNESS/ BAR(15,100),BB(100),BBDOT(100),PLOSS(2,100),
     *              XLONG(50),HTIME(2),IBAR(5,100),NL(2,100),
     *              NPTSPB(50),NPTPLY(50),NTHRNS(50),NBLTPH(50)
     *              ,FSCALE(50),FTYPI(50),FMU(50),RECTIM(50),DEL(50)
      DIMENSION FPREV(50),TPREV(50)
      F = 0.0
      ELOSS = 0.0
      IF(N.NE.1)GOTO99
C CALCULATE MUSCLE FORCES
C
C ACCOUNT FOR REACTION OR OTHER TIME DELAY
      TIME=XTIME-DEL(IM)
      IF(TIME.LE.O.)TIME=0.
C  MU RECRUITED LINEARLY FOR FIRST RECTIM SEC
      FN=TIME/RECTIM(IM)
      IF(FN.LE.O.O)FN=.001
C CHECK IF MU RECRUITMENT LEVEL IS EXCEEDED
      IF(FN.GE.FMU(IM)) FN=FMU(IM)
C CHECK IF MU RECRUITMENT EXCEEDS FRACTION OF TYPE I MU
      IF(FN.GE.FTYPI(IM))GOTO60
C CALCULATE AVERAGE CONTRACTION TIMES
      E5=EXP(5.*FN)*(5.*FN-1.)
      TC=.1-.011*(E5+1.)/FTYPI(IM)/(EXP(5.*FN)-1.)
      GOTO70
60    E5F=EXP(5.*FTYPI(IM))*(5.*FTYPI(IM)-1.)
      TC1=.1-.011*(E5F+1.)/FTYPI(IM)/(EXP(5.*FTYPI(IM))-1.)
      E5=EXP(5.*FN)*(5.*FN-1.)
      TC2=.01+.035/(1.-FTYPI(IM))
      TC3=.007/(1.-FTYPI(IM))*(E5-E5F)/(EXP(5.*FN)-EXP(5.*FTYPI(IM)))
      TC=TC1+TC2-TC3
C CALCULATE CONSTANT M FOR ACTIVE STATE FNC AND MAX STRAIN RATE (VEL)
70    FM=.372/TC
      EMAX=.297/TC
C CALCULATE PASSIVE SPRING FORCE
      FSP=.0016296*(EXP((7.6616*D)-1.))
C CALCULATE ACTIVE STATE FNC
      Q=32.53*(1.-EXP(-FM*TIME))**2.
      FQ=(.005+Q)/(1.+Q)
      R=RATE/EMAX
C CALCULATE LENGTH-TENSION RELATIONSHIP
      FL=.32+.71*EXP(-1.112*D)*SIN(3.722*(D+.34444))
C CALCULATE FORCE-VELOCITY RELATIONSHIP
      FV=.1433/(.1073+EXP(-1.409*SINH(3.2*R+1.6)))
C CALCULATE VISCOUS DAMPING FORCE
      FDAMP=.0
      IF(R.GT.0.)FDAMP=.138*R
C CALCULATE MAX MUSCLE FORCE
      FMAX=.00673**(1.-FN)
      F=(FSP+FQ*FL*FV+FDAMP)*FMAX
      IF(F.LE..15)GOTO75
C CALCULATE ENDURANCE TIME
      TEND=1236.5/(F*100.-15.)**.618 - 72.5
      IF(TEND.LE.6.9)TEND=6.9
      IF(TIME.LE.TEND)GOTO75
C IF TIME EXCEEDS ENDURANCE TIME, FORCE CAPABILITY IS REDUCED
      T=(TIME-TEND)/60.
```

```fortran
        F=F*(98.1-23.9*T+1.9*T*T)/100.
        IF(F.LE..15)F=.15
75      ELOSS = RATE*(FO*FL+FV)*FSCALE(IM)*FMAX
C GOLGI TENDON ORGAN RESPONSE (CLASP KNIFE REFLEX)
        IF(XTIME.EQ.0.)GOTO80
        DELT=TIME-TPREV(IM)
        IF(DELT.EQ.0.)GOTO98
        DELF=(F-FPREV(IM))/DELT
        WRITE(17,89)TIME,TPREV(IM),DELT,F,FPREV(IM),DELF
89      FORMAT(6F10.5)
        IF(DELF.GT.50.)F=0.
80      FPREV(IM)=F
        TPREV(IM)=TIME
        GOTO99
98      F=FPREV(IM)
99      F=F*FSCALE(IM)
        RETURN
        END
```

APPENDIX C

LISTING OF FORTRAN IV SOURCE DECK FOR
SUBROUTINE HINPUT

```
      SUBROUTINE HINPUT
C                                                             REV 6/30/35
C     CONTROLS THE INPUT OF CARDS F.8.A - F.8.D CONTAINING THE SETUP AND
C     CONTROL OF THE HARNESS BELT SYSTEM.
C
C
      IMPLICIT REAL*8(A-H,O-Z)
      COMMON/CONTRL/ TIME,NSEG,NJNT,NPL,NBLT, IAG,NVEH,NGRND,
     *               NS,NO,NSD,NFLX,NHRNSS,NWINDF,NJNTF,NPRT(36)
      COMMON/CNSNTS/ PI,RADIAN,G,THIRD,EPS(24),
     *               UNITL,UNITM,UNITT,GRAVIY(3)
      COMMON/HRNESS/ BAR(15,100),BB(100),BBDOT(100),PLOSS(2,100),
     *               XLONG(50),HTIME(2),IBAR(5,100),NL(2,100),
     *               NPTSPB(50),NPTPLY(50),NTHRNS(50),NBLTPH(50)
     *               ,FSCALE(50),FTYPI(50),FMU(50),RECTIM(50),DEL(50)
      COMMON/TABLES/MXNTI,MXNTB,MXTB1,MXTB2,NTI(50),NTAB(1250),TAB(6000)
      COMMON/CNTSRF/ PL(17,30),BELT(20,3),TPTS(6,8),BD(24,40)
      COMMON/TITLES/ DATE(3),COMENT(40),VPSTTL(20),BDYTTL(5),
     *               BLTTTL(5,8),PLTTL(5,30),BAGTIL(5,6),SEG(30),
     *               JOINT(30),CGS(30),JS(30)
      REAL DATE,COMENT,VPSTTL,BDYTTL,BLTTTL,PLTTL,BAGTIL,SEG,JOINT
      LOGICAL*1 CGS,JS
C     THIS COMMON/TEMTVS/ IS SHARED BY CINPUT, FINPUT, HINPUT AND FDINIT
      COMMON/TEMPVS/ JTITLE(5,51),NF(5),MS(3),KTITLE(31)
      REAL JTITLE,KTITLE
      IF  (NHRNSS.EQ.0)  GO TO 99
C
C     INPUT CARD F.8.A
C         (NOTE: NHRNSS NOW SUPPLIED ON INPUT CARD D.1)
C         NBLTPH - NO. OF BELTS PER HARNESS
C
      READ(15,11)  (NBLTPH(I),I=1,NHRNSS)
   11 FORMAT(18I4)
      WRITE(16,12) NHRNSS,(NBLTPH(I),I=1,NHRNSS)
   12 FORMAT('1 HARNESS-BELT SYSTEM INPUT',93X,'CARDS F.8'//
     *        '  NO. OF HARNESSES =',I4//
     *        '  NO. OF BELTS PER HARNESS =',50I2)
      J1 = 1
      K1 = 1
      DO 90 I=1,NHRNSS
      IF (NBLTPH(I).LE.0) GO TO 90
      J2 = J1 + NBLTPH(I) -1
C
C     INPUT CARD F.8.B - NPTSPB - NO. OF POINTS PER BELT.
C
      READ(15,17) (NPTSPB(J),J=J1,J2)
   17 FORMAT(10I4)
      WRITE(16,13) I,(NPTSPB(J),J=J1,J2)
   13 FORMAT('0 FOR HARNESS NO.',I3,' NO. OF POINTS PER BELT =',20I4)
      DO 30 J=J1,J2
      IF (NPTSPB(J).EQ.0) GO TO 30
C
C     INPUT CARD F.8.C - 5 FUNCTION NOS AND LENGTH OF EACH BELT.
C
      READ(15,14)NF,XLONG(J),FSCALE(J),FTYPI(J),FMU(J),RECTIM(J),DEL(J)
   14 FORMAT(5I4,F12.0,5F8.0)
C CHECK IF MUSCLE CHARACTERISTICS ARE REASONABLE
      IF(RECTIM(J).LT. .1)RECTIM(J)=.1
      IF(FTYPI(J).GE.100.)FTYPI(J)=99.99
      IF(FMU(J).LT.FTYPI(J))FMU(J)=FTYPI(J)
```

```
      IF(FMU(J).LE.30. .AND. FMU(J).GT.FTYPI(J)) FTYPI(J)=FMU(J)
      IF(FTYPI(J).LE.0.0) FTYPI(J)=.0001
      IF(NF(I).GE.0)WRITE(16,15) I,J,NF,XLONG(J),UNITL
   15 FORMAT('0 HARNESS NO.',I3,' BELT NO.',I3,' FUNCTION NOS.',5I6,
     *         '  REFERENCE SLACK = ',F9.3)
      IF(NF(I).LT.0)WRITE(16,19)I,J,FSCALE(J),
     *UNITM,FTYPI(J),FMU(J),RECTIM(J),DEL(J)
   19 FORMAT('0 MUSCLE NO.',I3,' SECTION NO.',I3,
     *'  MUSCLE FORCE SCALING FACTOR=',F8.2,1X,A4/
     *'    % SLOW TWITCH MU=',F8.2,'     % MU RECRUITED=',F8.2,
     *'   RECRUITMENT TIME=',F8.4,'   DELAY TIME=',F8.4)
      IF  (XLONG(J).EQ.0.0)  XLONG(J) = EPS(24)
      FTYPI(J)=FTYPI(J)/100.
      FMU(J)=FMU(J)/100.
      WRITE(16,16)
   16 FORMAT ('0   K    KS    KE    NT    NPD   NDR    FUNCTION NOS.',
     *          66X,'CARDS F.8.D'/)
C
C     SET UP POINTERS IN NTAB AND INITIAL VALUES OF TAB FOR BELT J
C         AS WAS DONE FOR OTHER CONTACTS IN SUBROUTINE FINPUT.
C
      NTHRNS(J) = MXNTB+1
      CALL FDINIT
      K2 = K1 + NPTSPB(J) - 1
      DO 70 K=K1,K2
C
C     INPUT CARD F.8.D
C
      READ(15,21) KS,KE,NPD,NDR,NF, (BAR(L,K),L=1,3)
   21 FORMAT (9I4,3F12.0)
      READ(15,22)  (BAR(L,K),L=7,12)
   22 FORMAT (6F12.0)
      IBAR(1,K) = KS
      IBAR(2,K) = KE
      IBAR(4,K) = NPD
      IBAR(5,K) = NDR
      IBAR(3,K) = MXNTB+1
      CALL FDINIT
      SQRER = 1.0
      IF  (KE.NE.0)  SQRER = DSQRT(XDY(BAR(1,K),BD(7,KE),BAR(1,K)))
      DO  26  L=1,3
      IF  (KE.NE.0)  BAR(L+6,K) = BD(L+3,KE)
   26 BAR(L+3,K) = BAR(L,K)/SQRER
      WRITE(16,31)  K,(IBAR(L,K),L=1,5),NF
   31 FORMAT (11I6)
   70 CONTINUE
      WRITE(16,71)  UNITL,UNITL,UNITL,UNITL
   71 FORMAT ('0',12X,'BASE REFERENCE (',     A4,')',
     *               7X,'ADJUSTED REFERENCE (', A4,')',
     *               11X,'OFFSET (',             A4,')',
     *               11X,'PREFERRED DIRECTION (',A4,')'/
     *         5X,'K',  4(8X,'X',8X,'Y',8X,'Z',3X) /)
      WRITE(16,72)  (K,(BAR(L,K),L=1,12),K=K1,K2)
   72 FORMAT (I6,3X,3F9.3,3X,3F9.3,3X,3F9.3,3X,3F9.3)
      K1 = K2+1
   80 CONTINUE
      J1 = J2+1
   90 CONTINUE
      DO  92  K=1,100
      BBDOT(K) = 0.0
```

```
      DO  91   J=1,2
91 PLOSS(J,K) = 0.0
      DO  92   J=1,3
92 BAR(J+12,K) = 0.0
99 RETURN
    END
```

APPENDIX D

REVISIONS TO

VALIDATION OF THE CRASH VICTIM SIMULATOR

VOL. 3 - USER'S MANUAL

APPENDIX D

REVISIONS TO
VALIDATION OF THE CRASH VICTIM SIMULATOR
VOL. 3 - USER'S MANUAL

D. SUBROUTINE SINPUT (p. 46)

NHRNSS   Number of harness-belt systems or active muscles to be
                          supplied on cards F.8.B-F.8.D. May be zero or blank.
                          Maximum value = 50. Note: In version 12 (for WPAFB)
                          this variable was supplied on card F.8.A.

F.8 Subroutine HINPUT - card input for harness-belt systems or active
     musculature (p. 69)

Note: NHRNSS which was supplied on card F.8.A for version 12 is now supplied on
card D.1. If NHRNSS #0, cards F.8 must be supplied. Previously for version 12,
a blank card F.8.A was required if no harness belt systems were desired.

CARD F.8.A   FORMAT (50I4) use three cards if NHRNSS > 18

    NBLTPH(I),   Number of individual belts for each harness No. 1. May
    I=1,NHRNSS   be zero or blank. Maximum value of sum of all NBLTPH is
                         50.

Card F.8.A is followed by NHRNSS sets of cards F.8.B - F.8.D.

Card F.8.B   Format (18I4) use two cards if NBLTPH(I) > 18.

    NPTSPB(J),   The number of reference points including anchor points
    J=1,NBLTPH(I)   for belt No. J of harness No. 1 may be zero or blank.
                         The maximum value of the sum of all NPTSPB for all
                         harness-belt systems is 100. The maximum value of the
                         sum of all NPTSPB for any one harness belt system is 50.
                         The maximum value of any individual NPTSPB is 25.

Each card F.8.B is followed by NBLTPH(I) sets of cards F.8.C - F.8.D

Card F.8.C   Format (5I4, F12.0, 5F8.0)

    NF(L),L=1   The function numbers from cards E.1 to define the
                         stress-strain of belt No. J. The definition of these
                         functions are identical to those of NF(1) to NF(5) on
                         cards F.2.B, except that the use of rate dependent
                         functions is permitted. NF(1) positive indicates a
                         harness while NF(1) negative indicates active
                         musculature. The function numbers are not used for the
                         active musculature.

    XI ONG(J)   The initial slack (IN) of belt No. J. A negative value
                         can be specified to indicate a pre-tightened belt. The
                         program will add this to the initial geometric length to
                         obtain the initial belt length and distribute the slack

D-1

proportionately between the points. For the active
musculature the slack is not needed (i.e., negative
strain is allowed) and can be left blank.

FSCALE(J)   Scaling used to multiply the normalized forces of each
                 muscle, equivalent to the maximum force the muscle can
                 produce.

FTYP1(J)   Percent of Type 1 motor units or muscle fibers in each
                 muscle. The value of FTYP1 must be equal to FMU for FMU
                 < 30% and less than or equal to FMU if FMU $\geq$ 30%.

FMU(J)   Percent of motor units recruited. FMU can vary from 0%,
                 or no muscle activity, to 100% or maximum voluntary
                 contraction.

RECTIM(J)   Time for full motor unit recruitment in seconds. RECTIM
                 must be greater than .1 sec found in ballistic
                 contractions.

DEL(J)   Delay time before motor unit recruitment in seconds.

APPENDIX E

ATB SPECIFICATIONS FOR HUMAN MUSCULATURE

ATB SPECIFICATIONS FOR HUMAN MUSCULATURE

Table 6. ATB Specifications for Elbow Musculature (Right Side Only)

Muscle Group	SEG	ORIGIN (in)			SEG	INSERTION (in)			Force Scaling Factor (lbs)
		X	Y	Z		X	Y	Z	
1) Biceps – Short Head	3	1.57	6.28	-3.24	13	.39	.0	-6.56	35.7
Brachii – Long Head	3	.0	6.28	-2.85	13	.39	.0	-6.56	42.4
2) Brachialis	12	.39	.0	-2.68	13	.39	.0	-7.15	101.86
3) Brachioradialis	12	.39	.39	3.61	13	.0	.79	.33	30.14
4) Triceps Medial Head	12	-.39	.0	- .72	13	-.59	.0	-8.53	116.9
Brachii Lateral Head	12	-.39	.0	-1.5	13	-.59	.0	-8.53	115.0
Long Head	3	.0	6.88	-1.85	13	-.59	.0	-8.53	128.4
5) Anconeus	12	.0	1.18	5.19	13	.39	.0	-6.94	20.68
6) Pronator Teres	12	.39	.0	4.35	13	.0	.71	-3.81	35.42
7) Supinator	12	.0	1.18	5.19	13	.0	.59	-5.94	38.94

Table 7. ATB Specifications for Shoulder Musculature (Right Side Only)

Muscle Group	SEG	ORIGIN (in)			SEG	INSERTION (in)			Scaling Factor (lbs)
		X	Y	Z		X	Y	Z	
1) Deltoid a)	3	-.79	6.49	-3.81	12	.39	.39	.07	121.11
b)	3	.79	6.49	-3.81	12	.39	.39	.07	121.11
2) Supraspinatus	3	.0	3.74	-1.85	12	.0	1.57	-5.83	72.6
3) Pectoralis a)	3	2.0	.0	-.28	12	.39	.39	-1.9	74.8
Major b)	3	2.0	3.34	-2.64	12	.39	.39	-1.9	74.8
4) Latissimus a)	2	-2.0	.0	3.85	12	.0	.39	-2.68	59.18
Dorsi b)	3	-2.0	.0	.71	12	.0	.39	-2.68	59.18
5) Teres Major	3	.0	4.92	2.09	12	.0	-.39	-3.08	109.34
6) Teres Minor	3	.0	5.71	.51	12	.0	.39	-5.44	34.54
7) Subscapularis	3	.39	4.92	.51	12	.59	.59	-5.44	217.8
8) Coraco Brachialis	3	1.57	7.28	-3.23	12	.0	-.39	-.72	33.44
9) Infraspinatus	3	-.39	4.52	-.28	12	.0	.59	-5.44	131.56

E-2

Table 8. ATB Specifications for Hip and Knee Musculature (Right Side Only)

Muscle Group		SEG	ORIGIN (in) X	Y	Z	SEG	INSERTION (in) X	Y	Z	Scaling Factor (lbs)
1)	Gluteus Medius	1	-1.46	.0	-2.23	6	-1.97	5.88	-8.21	465.96
2)	Gluteus Minimus	1	.0	.0	-1.44	6	-1.18	5.88	-8.21	211.2
3)	Tensor Fasciae Latae	1	-1.57	.0	-2.23	6	-1.97	5.49	-5.26	54.56
4)	Obturatus Internus	1	.0	1.95	3.68	6	-1.18	3.49	-8.88	86.02
5)	Adductor Longus	1	.0	.76	3.28	6	-1.18	4.7	-1.32	110.66
6)	Adductor Brevis	1	.0	1.55	3.68	6	-1.18	4.7	-3.09	99.88
7)	Adductor Magnus a)	1	.0	3.13	3.68	6	-1.18	4.7	-6.44	226.38
	b)	1	.0	1.55	3.68	6	-1.18	4.7	-8.8	226.38
8)	Pectineus	1	.787	1.55	.92	6	-1.18	1.0	-5.06	54.34
9)	Quadratus Femoris	1	-.79	1.95	3.68	6	-2.36	-1.97	-7.62	64.02
10)	Obturatus Externus	1	.0	1.95	3.68	6	-1.18	-1.97	-8.8	108.9
11)	Gluteus Maximus a)	1	.0	-3.15	-.65	6	-1.18	1.38	-4.47	323.62
	b)	1	.0	.0	.0	6	-1.18	1.38	-4.47	323.62
12)	Semimembranosus	1	-1.57	.0	2.49	7	.0	-1.18	-7.14	285.34
13)	Semitendinosus	1	-1.97	.0	2.49	7	.39	-.79	-4.39	95.26
14)	Biceps Femoris a)	1	-1.77	1.18	2.49	7	.0	1.57	-7.14	129.8
	b)	6	-1.18	1.18	-.53	7	.0	1.57	-7.14	129.8
15)	Quadriceps a)	1	.0	.0	-.23	7	1.18	.0	-7.93	308.0
	b)	6	.0	1.18	.65	7	1.18	.0	-7.93	924.0
16)	Iliopsoas a)	1	.0	-.39	3.41	6	-1.18	.79	-6.44	165.66
	b)	2	.0	.0	-.17	6	-1.18	.79	-6.44	165.66
17)	Gastrocnemius	6	.0	.0	8.52	8	.0	.0	-1.5	344.52
18)	Popliteus	6	-1.18	-1.57	9.7	7	-.79	.0	-5.57	43.78
19)	Gracilis	1	-.39	.76	3.67	7	.39	-.79	-5.17	35.86
20)	Sartorius	1	-1.57	.0	-1.05	7	.39	-.79	-5.17	34.1

Table 9 ATB Specifications for Neck Musculature (Right Side Only)

Muscle Group	SEG	ORIGIN (in) X	Y	Z	SEG	INSERTION (in) X	Y	Z	Scaling Factor (lbs)
1) Longus Capitis	4	-.75	1.0	-.54	5	1.54	.39	3.18	16.5
2) Rectus Capitis Anterior	4	-.75	1.0	-2.52	5	1.26	.39	3.18	5.5
3) Rectus Capitis Lateralis	4	-.75	1.0	-2.52	5	.87	1.18	3.18	5.5
4) Rectus Capitis Posterior Major	4	-.75	.0	-1.86	5	-.55	.94	2.83	11.0
5) Rectus Capitis Posterior Minor	4	-.75	.0	-2.52	5	-.55	.31	2.98	8.47
6) Obliquus capitis Superior	4	-.75	1.0	-2.52	5	-.55	1.38	2.67	22.0
7) Splenius Capitis	4	-.75	.0	2.16	5	-.39	1.57	2.67	26.84
8) Longissimus Capitis	4	-.75	1.0	2.16	5	.08	1.34	2.67	11.0
9) Spinalis Capitis	4	-.75	1.0	2.16	5	-.87	.24	2.83	11.0
10) Semispinalis Capitis	4	-.75	1.0	2.16	5	-1.42	.79	2.67	52.36
11) Trapezius	3	.0	7.28	-2.35	5	-1.42	.39	2.59	233.2
12) Sternocleido-Mastoideus	3	3.0	.0	-2.0	5	-.39	1.57	2.67	35.2
13) Levator Scapulae	3	-2.0	4.28	-1.85	2	-.31	.45	-1.85	390.5
14) Longus Colli	3	.75	.0	-2.0	4	.75	.0	-.18	16.5
15) Scalenus	3	3.0	2.0	-1.85	4	-.75	1.0	.2	38.5
16) Splenius Servicis	3	-.75	.0	-1.26	4	-.75	1.0	-1.86	15.4
17) Longissimus Servicis	3	-.75	1.0	-1.26	4	-.75	1.0	-.54	13.2
18) Spinalis Cervicis	3	-.75	.0	-2.6	4	-.75	.0	-1.86	27.5
19) SemiSpinalis Cervicis	3	-.75	1.0	-2.6	4	-.75	.0	-1.2	44.0
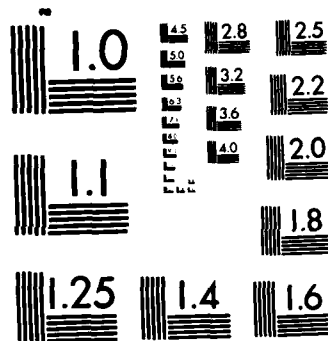
MICROCOPY RESOLUTION TEST CHART
NATIONAL BUREAU OF STANDARDS-1963-A

Table 10 ATB Specifications for Trunk Musculature (Right Side Only)

Muscle Group	SEG	ORIGIN (in) X	Y	Z	SEG	INSERTION (in) X	Y	Z	Scaling Factor (lbs)
1) Iliocostalis Lumborum	1	-1.0	1.5	3.85	2	-1.0	3.0	.31	22.0
2) Iliocostalis Dorsi	2	-1.0	3.0	.31	3	-1.0	3.0	.0	11.0
3) Longissimus Dorsi	2	-1.0	1.5	-.19	3	-.75	1.0	.71	22.0
4) Spinalis Dorsi	2	-1.0	.0	-4.23	3	-.75	1.0	.71	22.0
5) Semispinalis Dorsi	3	-.75	1.0	1.89	4	-.75	1.0	1.5	22.0
6) Multifidus a)	2	-1.0	1.5	-2.89	3	-.75	0	4.23	12.75
b)	3	-.75	1.0	-2.04	4	-.75	0	2.82	13.75
7) Interspinales a)	2	1.0	.0	-2.89	3	-.75	0	4.23	5.5
b)	3	-.75	.0	-2.04	4	-.75	0	2.82	5.5
8) Intertrans- Versarii a)	2	-1.0	1.5	-2.89	3	-.75	1.0	4.23	2.75
b)	3	-.75	1.0	-2.04	4	-.75	1.0	2.82	2.75
9) External Oblique	1	3.0	3.52	-3.08	2	.0	3.52	.31	150.7
10) Internal Oblique	1	.0	3.52	-3.08	2	3.0	3.52	.31	124.95
11) Rectus Abdominus	1	1.0	.5	1.92	3	3.0	.5	-4.23	58.52
12) Quadratus Lumborum	1	.0	3.52	-3.08	2	-.75	1.0	-.17	61.6

APPENDIX F

REFERENCES

APPENDIX F

REFERENCES

Alexander, R. S. and Johnson, P. D., Muscle Stretch and Theories of Contraction, Am. J. Physiol, 208:412-416, 1965.

Amis, A. A., Dowson, D. and Wright, V. "Elbow Joint Force Predictions for Some Strenuous Isometric Actions," J. Biom., 13:765-775, 1980.

An, K. N., Hui, F. C., Morrey, B. F., Linscheid, R. L. and Chao, E. Y. Muscles Across the Elbow Joint: A Biomechanical Analysis, J. Biom., 14:659-669, 1981.

Bawa, P., Mannard, A. and Stein, R. B. Predictions and Experimental Tests of a Visco-Elastic Muscle Model Using Elastic and Inertial Loads, Biol. Cybernetics, 22: 139-145, 1976.

Bigland, B. and Lippold, O. C. J. Motor Unit Activity in the Voluntary Contraction of Human Muscle, J. Physiol., 125:322-335, 1954.

Bland, D. R., The Theory of Linear Viscoelasticity, Pergamon Press, NY, 1960.

Butler, F. E. and Fleck, J. T., Advanced Restraint System Modelling, AFAMRL-TR-80-14, Wright-Patterson AFB, OH, 1980.

Caldwell, L. S. Relative Muscle Loading and Endurance, J. Engr. Psychol., 2:155-161, 1963.

Caldwell, L. S. The Load-Endurance Relationship for a Static Manual Response, Human Factors, 6:71-79, 1964.

Chao, E. Y. and Morrey, B. F. Three Dimensional Rotation of the Elbow, J. Biom., 11:57-73, 1978.

Clamann, H. P. Activity of Single Motor Units During Isometric Tension, Neurology, 20:254-260, 1970.

Close, R. I. The Relation between Intrinsic Speed of Shortening and Duration of the Active State of Muscle, J. Physiol., 180:542-559, 1965.

Close, R. I. Dynamic Properties of Mammalian Skeletal Mucles, Physiol. Rev., 52:129-196, 1972.

Crowninshield, R. D., Johnston, R. C., Andrews, J. G. and Brand, R. A. A Biomechanical Investigation of the Human Hip, J. Biom., 11:75-86, 1978.

deLuca, C. J. and Forrest, W. J. Force Analysis of Individual Muscles Acting Simultaneously on the Shoulder Joint During Isometric Abduction, J. Biom., 6:385-393, 1973.

Dempster, W. T. Mechanisms of Shoulder Movement, Arch. Phys. Med. and Rehab., 46:49-69, 1965.

Desmedt, J. E. and Godaux, E. Ballistic contractions in man: Characteristic recruitment pattern of single motor units of the tibialis anterior muscle, J. Physiol, 264:673-693, 1977.

Desmedt, J. E. and Godaux, E. Ballistic contractions in fast or slow human muscles; discharge patterns of single motor units, J. Physiol, 285:185-196, 1978.

Dostal, W. G. and Andrews, J. C. A Three Dimensional Biomechanical Model of Hip Musculature, J. Biom., 14:803-812, 1981.

Ebashi, S. and Endo, M. Calcium Ion and Muscular Contraction, Progr. Biophys. Mol. Biol., 18:125-183, 1968.

Engin, A. E. On the Biomechanics of the Shoulder Complex, J. Biom., 13:575-590, 1980.

Fick, R. Handbuch der Anatomie and Mechanik der Gelenke unter Ber Ücksichtigung der bewegenden Muskeln, Jena, Germany; Fischer, 1910.

Fleck, J. T. Calspan Three-Dimensional Crash Victim Simulation Program, Aircraft Crashworthiness, University Press of Virginia, 1975.

Fleck, J. T. and Butler, F. E. Development of an Improved Computer Model of the Human Body and Extremity Dynamics, AFAMRL-TR-75-14, Wright-Patterson AFB, OH, 1975.

Fleck, J. T. and Butler, F. E. Validation of the Crash Victim Simulator, Final Report No. ZS-5881-V-4,Calspan Corp. 1982, 4 vols.

Fleck, J. T., Butler, F. E. and Vogel, S. L. An Improved Three Dimensional Computer Simulation of Motor Vehicle Crash Victims, Final Technical Report No. ZQ-5180-L-1, Calspan Corp., 1974, 4 Vols.

Flügge, W., Viscoelasticity, Blaisdell Pub. Co., Waltham, Mass, 1967.

Freivalds, A. Modelling of an Active Neuromuscular Response to Mechanical Stress, Final Report USAF Contract No. F49620-82-C-0035, Wright-Patterson AFB, OH, 1984.

Freivalds, A. Advanced Development of an Active Neuromuscular Response to Mechanical Stress, Final Report for AFOSR Contract No. 83-0106, 1984.

Freivalds, A. and Kaleps, I. Modelling of Active Neuromuscular Response to Dynamic Mechanical Stresses, Proceedings of the Institute of Industrial Engineers, pp. 196-198, 1983.

Freivalds, A. and Kaleps, I. Computer-Aided Strength Prediction Using the Articulated Total Body Model, Computers & Industrial Engineering, 8:107-118, 1984.

Fung, Y. C., Biomechanics, Mechanical Properties of Living Tissues, Springer-Verlag, NY, 1981.

Glantz, S. A. A Constitutive Equation for the Passive Properties of Muscle, J. Biomech., 7:137-145, 1974.

Glantz, S. A. A Three-Element Description for Muscle With Viscoelastic Passive Elements, J. Biomechanics, 10:5-20, 1977.

Granit, R. The Basis of Motor Control, Academic Press, NY, 1970.

Granit, R. and Pompeiano, O. (eds) Reflex Control of Posture and Movement, (Vol. 50 of Progress in Brain Research), Elsevier/North Holland Biomedical Press, N.Y. 1979.

Gray, H., Pick, T. P. and Howden, R. Anatomy, Descriptive and Surgical, (Reprint of 1901 Edition of Gray's Anatomy) Running Press, Philadelphia 1974.

Hatze, H. A Theory of Contraction and a Mathematical Model of Striated Muscle, J. Theoret. Biol., 40:219-246, 1973.

Hatze, H. A. Myocybernetic Control Model of Skeletal Muscle, Biol. Cybernetics, 25:103-119, 1977.

Hatze, H. A Teleological Explanation of Weber's Law and the Motor Unit Size Law," Bull. Mathem. Biol., 41:407-425, 1979.

Hatze, H. Myocybernetic Control Models of Skeletal Muscle, University of South Africa, Pretoria, 1981.

Henneman, E. and Olson, C. B. Relations Between Structure and Function in Design of Skeletal Muscle, J. Neurophysiol., 28:581-598, 1965.

Houk, J. and Henneman, E. Feedback Control of Skeletal Muscles, Brain Res. 5:433-451, 1967.

Huxley, H. E. Electron Microscope Studies of the Organization of Filaments in Striated Muscle, Biochem. Biophys. Acta, 12:387, 1953.

Ikai, M. and Fukunaga, T. Calculation of Muscle Strength per Unit Cross-sectional Area of Human Muscle by Means of Ultrasonic Measurement, Int. Z. Angew. Physiol. einschl. Arbeitsphysiol., 26:26-32, 1968.

Jensen, R. H. and Davy, D. T. An Investigation of Muscle Lines of Action About the Hips: A Centroid Line Approach vs. Straight Line Approach, J. Biom., 8:103-110, 1975.

Kogi, K. and Hakamada, T. Slowing of Surface Electromyogram and Muscle Strength in Muscle Fatigue, Institute for Science of Labor Reports, Tokyo, Japan, No. 60, 1962.

Kroemer, K. H. E. Human Strength, Terminology, Measurement, and Interpretation of Data, Human Factors, 12:297-313, 1970.

MacConaill, M. A. The Movement of Bones and Joints - II Function of the Musculature, J. Bone & Surgery, 31B:100-104, 1949.

McMinn, R. M. H. and Hutchings, R. T. Color Atlas of Human Anatomy, Yearbook Medical Publishers, Chicago, IL, 1977.

Merchant, A. C. Hip Abductor Muscle Force, J. Bone and Jt. Surg., 47A:462-476, 1965.

Milner-Brown, H. S., Stein, R. B. and Yemm, R. The Orderly Recruitment of Human Motor Units During Voluntary Isometric Contractions, J. Physiol., 230:359-370, 1973a.

Milner-Brown, H. S., Stein, R. B. and Yemm, R. Changes in Firing Rate of Human Motor Units During Voluntary Isometric Contractions, J. Physiol., 230:371-390, 1973b.

Minns, R. J. Forces at the Knee Joint, Anatomical Considerations, J. Biom., 9:633-643, 1981.

Monod, H. and Scherrer, J. The Work Capacity of a Synergic Muscular Group, Ergonomics, Vol. 8:329-338, 1965.

Müller, E. A. Das Arbeitsmaximum bei Statischer Haltearbeit, Arbeitsphysiol. 5:605-612, 1932.

Nissan, M. Review of Some Assumption in Knee Biomechanics, J. Biom. 12:375-381, 1980.

Parmley, W. W., Yeatman, L. A. and Sonnenblick, E. H. Differences Between Isotonic and Isometric Force Velocity Relationships in Cardiac Skeletal Muscle, Am. J. Physiol. 219:546-550, 1970.

Person, R. and Kudina, L. P. Discharge Frequency and Discharge Pattern of Human Motor Units During Voluntary Contraction of Muscle, Electroenceph Clin Neurophysiol. 32:471-483, 1972.

Petrofsky, J. S. Isometric Exercise and Its Clinical Implications, C. C. Thomas, Springfield, IL. 1982.

Quiring, D. P. Boyle, B. A., Boroush, E. L. and Lufkin, B. The Extremities, Lea & Febiger, Philadelphia, 1945.

Quiring, D. P. The Head, Neck and Trunk, Lea & Febiger, Philadelphia, 1947.

Rab, G. T. Muscle Forces in the Posterior Thoracic Spine, Clin. Orthoped., 139:28-32,1979.

Rab, G. T., Chao, E. Y. S. and Stauffer, R. N. Muscle Force Analysis of the Lumbar Spine, Orthop. Clincis of North Amer., 8:193-199, 1977.

Rohmert, W. Ermittlung von Erholungspausen für Statische Arbeit des Menschen, Int. Z. Angew. Physiol. einschl. Arbeitsphysiol., Vol. 18:123-164, 1960.

Schmidt, R. E. Fundementals of Neurophysiology, N. Y. Springer-Verlag, N. Y. 1975.

Schumacher, G. H. and Wolff, E. Trockengewicht and Physiologischer
Querschnitt der Menschlichen Skelettmuskulatur, II, Physiologische
Querschnitte, <u>Anat. Anz.</u>, 119:259-269, 1966.

Schutz, R. K. <u>Cyclic Work-Rest Excercises Effect on Continuous Hold Endurance
Capacity</u>, Ph.D. Dissertation, University of Michigan, Ann Arbor, MI, 1972.

Seireg, A. and Arvikar, R. J. A Mathematical Model for Evaluation of Forces
in Lower Extremities of the Musculo-skeletal System, <u>J. Biom.</u>, 6:313-326,
1973.

Smidt, G. L. Biomechanical Analysis of Knee Flexion and Extension, <u>J. Biom.</u>,
6:79-92, 1973.

Stephens, J. A. and Usherwood, T. P. The Mechanical Properties of Human Motor
Units with Special Reference to Their Fatigability and Recruitment Threshold,
<u>Brain Res.</u>, 125:91-97, 1977.

Takashima, S. T., Singh, S. P., Harderspeck, K. A. and Schultz, A. B. A Model
for Semi-quantitative Studies of Muscle Actions, <u>J. Biom.</u>, 12:929-939, 1979.

Tanji, J. and Kato, M. Firing Rate of Individual Motor Units in Voluntary
Contraction of Abductor Digiti Minimi Muscle in Man, <u>Experimental Neurology</u>,
40:771-783, 1973.

Williams, J. and Belytschko, T. <u>A Dynamic Model of the Cervical Spine and
Head</u>, AFAMRL-TR-81-5, Wright-Patterson AFB, OH, 1981.

Wismans, J., Veldpaus, F., Janssen, J., Huson, A. and Struben, P. A Three
Dimensional Mathematical Model of the Knee Joint, <u>J. Biom.</u>, 13:677-685, 1980.

Youm, Y., Dryer, R. F., Thambyrajah, K., Flatt, A. E. and Sprague, B. L.
Biomechanical Analyses of Forearm Pronation-supination and Elbow
Flexion-extension, <u>J. Biom.</u>, 12:245-255, 1979.

END

FILMED

2-86

DTIC